

# The Molonglo Southern 4 Jy Sample (MS4). I. Definition

A. M. Burgess<sup>1</sup>

annb@psych.usyd.edu.au

and

R. W. Hunstead

*School of Physics, University of Sydney, NSW 2006, Australia*

rwh@physics.usyd.edu.au

## ABSTRACT

We have defined a complete sample of 228 southern radio sources at 408 MHz with integrated flux densities  $S_{408} > 4.0$  Jy, Galactic latitude  $|b| > 10^\circ$  and declination  $-85^\circ < \delta < -30^\circ$ . The main finding survey used was the Molonglo Reference Catalogue. We describe in detail how the Molonglo Southern 4 Jy sample (MS4) was assembled and its completeness assessed. Sources in the sample were imaged at 843 MHz with the Molonglo Observatory Synthesis Telescope to obtain positions accurate to about  $1''$ , as well as flux densities and angular sizes; follow-up radio and optical observations are presented in Paper II. Radio spectra for the MS4 have been compiled from the literature and used to estimate flux densities at 178 MHz. The strong-source subset of MS4, with  $S_{178} > 10.9$  Jy (SMS4), provides a southern sample closely equivalent to the well-studied northern 3CRR sample. Comparison of SMS4 with 3CRR shows a reassuring similarity in source density and median flux density between the two samples.

*Subject headings:* radio continuum: galaxies — galaxies: active — surveys

---

<sup>1</sup>present address: School of Psychology, University of Sydney, NSW 2006, Australia.

## 1. INTRODUCTION

Well defined, complete surveys are essential starting points for learning about the global characteristics of astronomical sources. At radio frequencies, the easiest way to select a large, well defined sample is to choose all objects brighter than a given flux density at a given observing frequency. Such a sample has the advantage of containing the objects with the highest signal-to-noise ratio. Because any one finding survey is likely to be affected either by confusion or by over-resolution for some of the sources, it is often necessary to use more than one survey to define a flux density-limited sample. Even then the sample may not be complete, but may, for example, be missing sources (or portions of sources) of low surface brightness or very large angular size.

One of the best studied radio samples in the past few decades has been the northern hemisphere Third Cambridge Catalogue (3C; Edge et al. 1959) and its revised versions the 3CR (Bennett 1962) and 3CRR (Laing et al. 1983). Being selected at low frequency (159 and later 178 MHz), it contains a large proportion of extended, steep-spectrum sources. Because of the high flux-density limit ( $S_{178}$ ) of around 11 Jy, the sample contains a large proportion of very powerful sources. The most complete version, the 3CRR, is the one discussed in this paper.

As so many studies of high-power radio sources have been based on this one sample, it is essential to have a comparison sample to test whether the 3CRR is truly representative. This paper is concerned with the definition of such a comparison sample, selected at low frequency to have properties similar to 3CRR. Increasing the sky coverage is more important at high flux densities where the total number of sources is limited. This sample was selected at 408 MHz to contain the  $\sim 200$  brightest extragalactic objects south of  $\delta = -30^\circ$ .

The sample is defined in Section 2. Follow-up observations of the whole sample with the Molonglo Observatory Synthesis Telescope at 843 MHz are described in Section 3. These observations have provided more accurate positions and angular sizes, as well as flux densities in a gap in the radio spectrum. The definition of a strong subsample at 178 MHz, for comparison with 3CRR, is described in Section 4. In Paper II (Burgess & Hunstead 2006) we present follow-up imaging at 5 GHz of the more compact sources with the Australia Telescope Compact Array, together with optical identifications using the UK Schmidt sky survey and CCD images from the Anglo-Australian Telescope.

## 2. DEFINITION OF THE MS4 SAMPLE

Our motivation was to generate a sample of strong southern radio sources for comparison with (and extension of) the well studied northern 3CRR sample. For reference, Table 1 contains a summary of southern finding surveys of strong sources. Our selection frequency of 408 MHz (as opposed to 178 MHz used for 3CRR) was chosen because it allowed the sources to be selected from the Molonglo Reference Catalogue (MRC; Large et al. 1981), the deepest and most complete low-frequency survey of the southern sky. The flux-density limit of 4.0 Jy was chosen to give a useful but manageable number of sources,  $\sim 200$ –250. The sample is therefore called the Molonglo Southern 4 Jy sample, abbreviated as MS4.

The selection criteria for the MS4 sample are as follows:

- (i) Declination  $-85^\circ < \delta < -30^\circ$ .
- (ii) Flux density  $S_{408} > 4.0$  Jy.
- (iii) Galactic latitude  $|b| > 10^\circ$ .
- (iv) Not in the Magellanic Cloud regions.
- (v) Not a known Galactic source.

The reason for excluding the small area south of  $-85^\circ$  is that the MRC is incomplete in this region. At least one source would otherwise be in the sample: PKS B0349–88, with  $S_{408} = 6.8$  Jy (Price & Milne 1965). The northern limit of  $\delta = -30^\circ$  was chosen to preserve a reasonable beamshape for follow-up images made with the east-west arrays of the Australia Telescope Compact Array (ATCA) and Molonglo Observatory Synthesis Telescope (MOST). For the purposes of sample definition the original B1950 coordinates were retained, but all positions are given for the J2000 equinox.

The Galactic Plane and Magellanic Cloud regions are excluded for two reasons: the strong radio emission from local sources makes background extragalactic objects hard to recognise, and the dust obscuration and high star density make optical identifications difficult. The Magellanic Cloud regions are those defined by Turtle & Amy (1991), i.e.,  $00^{\text{h}}25^{\text{m}} < \alpha < 01^{\text{h}}35^{\text{m}}$ ,  $-74^\circ40' < \delta < -70^\circ45'$  for the Small Magellanic Cloud, and  $04^{\text{h}}46^{\text{m}} < \alpha < 05^{\text{h}}58^{\text{m}}$ ,  $-72^\circ20' < \delta < -65^\circ10'$  for the Large Magellanic Cloud. Examination of the 408 MHz MC4 survey (Clarke et al. 1976) reveals that the only sources in these regions with  $S_{408} > 4.0$  Jy are associated with the Clouds rather than being background objects. From the mean source density of MS4 (§ 2.6) we would expect only two sources to lie in these regions, so a count of zero is not surprising.

## 2.1. The Molonglo Cross Telescope and the Molonglo Reference Catalogue

The Molonglo Reference Catalogue (MRC) was compiled from data taken between 1968 and 1978 with the Molonglo Cross Telescope. This telescope was a Mills Cross interferometer operating at 408 MHz with a bandwidth of 2.5 MHz, and resolution of  $2.67' \times 2.86' \sec(\delta + 35^\circ.4)$  (Mills et al. 1963). The flux-density calibration (Hunstead 1991) was based on the absolute scale of Wyllie (1969a) and the pencil-beam sensitivity curve measured by Hunstead (1972). The survey for the MRC covered the declination range  $-85^\circ \leq \delta \leq +18^\circ.5$ , with Galactic latitude  $|b| > 3^\circ$ . The MRC contains 12141 sources above its lower flux-density limit of  $S_{408} = 0.7$  Jy, and contains 7347 sources above its notional completeness level of 1 Jy. As well as positions and flux densities, the catalogue contains cross-references to other catalogues, and some structural information for extended sources. For sources stronger than 4 Jy the positional errors are around  $3''$  in  $\alpha$  and  $4''$  in  $\delta$ , and the standard error in flux density is around 4%.

In defining our sample, we used the MRC in preference to the two previous extensive low-frequency surveys of the southern sky, the Mills, Slee, and Hill (MSH) survey at 85.5 MHz (Mills et al. 1958, 1960, 1961) and the Parkes 408 MHz catalogues (Bolton et al. 1964; Price & Milne 1965). Compared with the MRC, the MSH and Parkes catalogues have less uniform sky coverage, lower sensitivity, and higher source confusion due to lower resolution. Of the 228 sources in the MS4 sample, 43 were not in the original Parkes survey: of these, 35 were in the region of sky covered by that survey. Because of their much wider beams, the Parkes and MSH surveys were valuable in providing integrated flux densities for strong but very extended sources (such as the lobes of Centaurus A) which are substantially resolved out by the Molonglo Cross.

## 2.2. Initial Selection of the Sample

Initial selection of the MS4 sample from the MRC gave 215 sources in the region of interest with  $S_{408} > 4.0$  Jy. This list was refined using the study of Jones & McAdam (1992), hereafter referred to as JM92. They used the Molonglo Observatory Synthesis Telescope (MOST) to image at 843 MHz all MRC sources south of  $-30^\circ$  which were flagged as extended or multiple. Their higher resolution MOST images made it possible to distinguish between genuine extended sources, some with more than one MRC entry, and close groups of unrelated sources. Following Jones (1989b), two MRC sources were considered to be parts of a single source if they were extended towards each other, or if they were connected at or above the 2% contour level. This latter criterion corresponds to a separation of about  $105''$  for two unresolved sources. For instance, we excluded MRC B0230–666, with  $S_{408} = 4.39$  Jy, from

our sample because JM92 show it is composed of two separate compact sources, each well below our 4 Jy limit. MRC B1459–417, identified with the Galactic supernova remnant SNR 1006 (Stephenson et al. 1977), was also excluded. After excluding these two sources, and counting 5 sources with multiple MRC entries only once, our sample contained 208 sources. This was, however, still incomplete, because of the underestimation of flux densities of extended sources in the MRC.

The MRC flux densities were calculated using a point-source fitting algorithm which is reliable for sources with angular extent less than  $\sim 1'$ . For larger angular sizes the fitted value underestimates the integrated flux density, so it was necessary to estimate the integrated  $S_{408}$  for each extended source in the region of interest. We first obtained a candidate list of 178 sources with MRC flux densities between 1 and 4 Jy, and flagged as extended or multiple; weaker sources were ignored as the MRC is incomplete below 1 Jy. Of the 178 sources, 97 were found by JM92 to have largest angular size  $> 1'$ . We searched the literature for flux-density measurements at 408 MHz for these 97 sources. If such measurements were unavailable, we used the radio spectrum or unpublished Molonglo 408 MHz data. As a result of these estimates, described in the following section, 20 extended sources were added to the sample, bringing the total number of sources to 228.

## 2.3. Flux Densities of Extended Sources

### 2.3.1. Published Flux Densities at 408 MHz

408 MHz flux densities for extended southern sources are available from either the 64 m Parkes Telescope or the Molonglo Cross. The Molonglo papers used the absolute flux-density scale of Wyllie (1969a), whereas the Parkes catalogues used the scale of Conway et al. (1963), which was nominally about 10% lower. However, Wyllie (1969b) found a mean ratio  $\langle \text{Molonglo/Parkes} \rangle = 1.000 \pm 0.015$  and we have therefore not made any adjustments to the Parkes flux densities.

The main Parkes 408 MHz data were collected as part of the original Parkes surveys (Bolton et al. 1964; Price & Milne 1965). The Parkes beam size of  $48'$  often led to over-estimation of flux densities because of confusing sources in the beam. We therefore used these flux densities only if estimates via the radio spectrum (§ 2.3.2) were unavailable, or for strong sources where confusion was unlikely to be severe. Parkes 408 MHz flux densities were used to exclude four sources from the sample. Few of the remaining candidates were in the Parkes catalogue, as they lay well below its stated completeness limit of 4 Jy.

The two main sets of Molonglo Cross data in the region of interest were those of Schilizzi

& McAdam (1975), hereafter referred to as SM75, and the MC4 survey of the Magellanic Cloud regions (Clarke et al. 1976). SM75 estimated integrated 408 MHz flux densities for 116 sources found to be extended with Parkes or Molonglo. A total of 17 candidates from our list were in their survey, of which 11 were listed as having  $S_{408} > 4.0$  Jy. One of these candidates, MRC B2130–538, in the cluster Abell 3785, was subsequently excluded because a high-resolution image (Haigh 2000), made with the Australia Telescope Compact Array at 20 cm, showed it to be two independent radio sources. We also included a source, PKS B1400–33, which had  $S_{408} > 4.0$  Jy in SM75, but did not appear in the MRC.

The MC4 finding survey covered the Magellanic Clouds, as well as comparison regions in the declination range  $-61^\circ \leq \delta \leq -75^\circ$ . Of the 10 candidates observed in this survey, two were found to have integrated flux density  $S_{408} > 4.0$  Jy.

Integrated flux densities at 408 MHz measured with the Molonglo Cross by J. Rathmell (Ekers et al. 1989) were used to include MRC B1056–360, with  $S_{408} = 4.09$  Jy.

### 2.3.2. *Estimates from the Radio Spectrum*

Because extended sources usually have power-law radio spectra, it is often possible to estimate flux densities by linear interpolation or extrapolation of a  $\log S_\nu$ :  $\log \nu$  plot. We used flux-density measurements at other frequencies to estimate  $S_{408}$  for sources without published integrated flux densities at 408 MHz. It was sometimes necessary to extrapolate to  $S_{408}$ , if data at lower frequencies were unavailable. There will be systematic error in these estimates both from missing flux density for sources with large angular extent, and from confusion in low-resolution observations, in particular those of MSH at 85.5 MHz, and Parkes at 408 and 1410 MHz.

To quantify the error in the flux-density estimates, we compared flux densities from SM75 with values interpolated or extrapolated from the radio spectrum for 20 extended sources. For 15 of these sources, the estimate from the radio spectrum was larger than the SM75 value. For the 8 sources with largest angular size  $LAS < 7'$ , the median flux-density difference was 13%, and for the 12 sources with  $LAS \geq 7'$  the median flux-density difference was 24%. These systematic differences are attributed to the limited surface brightness sensitivity of the  $3'$  Molonglo Cross pencil beam.

On the basis of the radio spectra, two sources were added to the sample.

### 2.3.3. *Estimates from Unpublished Molonglo 408 MHz Data*

The unpublished Molonglo Transit Catalogue, from an intermediate stage in the compilation of the MRC, contains estimates of integrated flux densities which we were able to compare with the corresponding values in SM75. The Transit Catalogue values were found to underestimate the total flux density for sources of  $\text{LAS} \gtrsim 6'$ . For sources with a single MRC entry and  $\text{LAS} < 6'$  the estimates were reliable. Of the 21 sources in this latter category, four were added to the sample.

After performing these various estimates of  $S_{408}$ , we were left with 20 extended MRC sources to add to the MS4 sample. They are listed in Table 2. Extended sources with integrated flux densities just below the 4.0 Jy cutoff are listed in Table 3.

## 2.4. Completeness

### 2.4.1. *Systematic Errors*

In spite of the work described in Section 2.3, the MS4 sample may still be incomplete, due to very extended sources. Since the MRC is complete only for sources with fitted flux density  $> 1$  Jy, we may be missing some strong but diffuse sources with surface brightness  $< 1$  Jy/beam. However, such sources should have been catalogued in the lower resolution Parkes surveys, and a search in the region of interest for non-MRC sources with  $S_{408} > 4.0$  Jy located only three objects. Two of these, PKS B1209–52 and PKS B1210–52, are part of the Galactic supernova remnant G296.5+10.0 (Whiteoak & Gardner 1968), and have not been included. The third, PKS B1400–33, is a low-surface-brightness possible relic radio source associated with the weak cluster around NGC 5419 (Goss et al. 1987; Subrahmanyan et al. 2003); this source was measured by SM75 and has been included in the MS4 sample.

The Parkes surveys did not have a uniform cutoff in Galactic latitude, and missed some regions with  $|b| > 10^\circ$ . These excluded regions, however, occupy only a small fraction of the sky south of  $-30^\circ$  (Ekers 1969a, Figure 1), and given the rarity of sources as diffuse as PKS B1400–33, it is unlikely that any other low-surface-brightness sources have been overlooked.

Completeness may be affected by the accidental omission of extended sources with components listed separately in the MRC. A giant source with compact lobes separated by  $> 8'$  would have no extension flag in the MRC, and would not be in our list of extended candidates. There are several giant radio galaxies in Table 2, and we estimate that very few, if any, have been missed.

Errors in estimating  $S_{408}$  from the radio spectrum may affect completeness, particularly for values relying on extrapolation. The 843 MHz integrated flux densities of JM92 were later found to be systematically low (see Section 3.4) by 6%; this could, in principle, lead to an extrapolated  $S_{408}$  for a genuine 4 Jy source being reduced below the sample limit. Extended sources falling just below the sample limit are listed in Table 3.

#### 2.4.2. Random Errors

The sample content may also be biased by random errors in the flux density measurements, as some sources with measured  $S_{408} > 4.0$  Jy may have true flux densities  $< 4.0$  Jy, and vice versa. Because the differential source counts have a negative slope near 4 Jy, slightly more sources will be wrongly included in the sample than will be wrongly excluded from it (Jauncey 1968). We estimated the number of sources likely to be affected by considering the flux densities and flux density errors of all MRC sources in the region of interest with measured flux densities between 1 and 10 Jy. Assuming the MRC flux-density errors were Gaussian, we calculated the expected number of sources with measured  $S_{408}$  between 4 and 10 Jy but true  $S_{408} < 4.0$  Jy to be 6.1. Similarly we calculated the expected number of sources with measured  $S_{408}$  between 1 and 4 Jy but true  $S_{408} > 4.0$  Jy to be 5.7.

The net number of sources wrongly included is therefore  $< 1$ , so we can be confident that the sample *size* is not affected, although the sample *content* is not quite the same as it would be for zero measurement error. As the MRC errors are not actually Gaussian but have a long tail (Large et al. 1981), the numbers of sources thus brought into and taken out of the sample may be slightly larger than estimated here.

#### 2.4.3. Variability

Flux-density variability can also cause a bias in sample content, but as the MS4 contains comparatively few flat-spectrum sources, only a small fraction of the sample can be affected by variability. While 30–50% of flat-spectrum sources are variable at 408 MHz (Mantovani et al. 1992), less than 2% of steep-spectrum sources vary at low frequency (Dennison et al. 1981; Mantovani 1982). As only 14 of the 228 MS4 sources have flat radio spectra ( $\alpha \geq -0.5$ , defined in the sense  $S_\nu \propto \nu^\alpha$ ), fewer than 5% of all MS4 sources are likely to vary significantly at 408 MHz. Consequently the effects of variability on sample size have been ignored.



#### 2.4.4. Summary

In summary, problems of incompleteness are likely to affect the net sample size only for extended sources. Fewer than five extended MRC sources are likely to have been wrongly excluded from the MS4 sample because of systematic underestimates of their flux densities. From examination of the lower resolution Parkes 408 MHz surveys, few if any sources have been excluded through not being in the MRC. When the survey with the Mauritius radio telescope (Golap et al. 1998) at 151.5 MHz has been analysed, it will provide an extra point in the radio spectrum to verify  $S_{408}$  for extended sources north of  $\delta = -70^\circ$ .

### 2.5. Comparison with the Northern Sample of Best et al. (1999)

A sample similar to the MS4 has been defined from the MRC to have  $S_{408} > 5$  Jy in the declination range  $-30^\circ \leq \delta \leq +10^\circ$  (Best et al. 1999, hereafter BRL99). Although containing useful radio and optical data, the BRL99 sample has the disadvantage — for statistical studies — of radio incompleteness, as it was defined purely from the MRC flux densities, without examining those extended sources with MRC flux densities below 5 Jy.

To assess the number of sources likely to be missing from the BRL99 sample, we used the flux densities of the MS4 sample. In total, 160 MS4 sources had integrated  $S_{408} > 5$  Jy; of these 15 were extended sources with  $S_{408} < 5$  Jy in the MRC. The median angular size of these 15 sources was  $450''$  and the minimum angular size was  $126''$ . These sources form around 10% of the MS4 sample with  $S_{408} > 5$  Jy. We would expect a similar fraction to be missing from the BRL99 sample. The incompleteness is most likely to affect their sample at low redshifts, as they predict. We note that of the 15 MS4 sources  $\geq 5$  Jy which would have been excluded by the BRL99 selection criteria, 14 have  $z < 0.2$ . This deficit is evident in the lowest redshift bin of Figure 53 of BRL99, and will necessarily compromise studies of the local radio luminosity function using this sample.

In assessing the completeness of their sample, BRL99 have misguidedly used the PKSCAT90 compilation (Otrupcek & Wright 1991) rather than the original Parkes catalogues (Bolton et al. 1964; Shimmins et al. 1966; Day et al. 1966). Most of the 408 MHz flux densities listed by PKSCAT90 are not Parkes measurements at all, but are taken directly from the MRC. This explains the large number of data points in Figure 52 of BRL99 for which *exactly* 100% of the so-called “Parkes flux density” is contained in the MRC value. Unfortunately, there is no rationale given by the compilers of PKSCAT90 for when they chose to use MRC rather than Parkes data. The puzzling bimodal distribution in Figure 52 of BRL99 for angular sizes greater than  $100''$  suggests that the decision was *not* related to angular size. As a result,

flux densities, spectral indices, and radio powers for large angular size sources in Table 2 of BRL99 will be unreliable.

## 2.6. The MS4 Sample

The sample contains 228 sources, and is summarised in Table 4. The columns of this table are as follows:

1. MRC name.
2. Parkes name. If there are two digits of declination this is from the original Parkes catalogue (Bolton et al. 1964; Price & Milne 1965), and if three digits, from the Parkes 2700 MHz catalogue (Bolton et al. 1979 and references therein).
3. Name of the source as given in the 85.5 MHz MSH survey (Mills et al. 1960, 1961).
4. 408 MHz flux density. This is usually from the MRC but for some extended sources is taken from other 408 MHz measurements or estimated from the radio spectrum (see Section 2.3). References are given in Column 6 of Table 5.
5. References to radio images in the literature, excluding VLBI images.

The sample covers an area of 2.43 sr, with a source density of  $94 \text{ sr}^{-1}$ , compared with the 3CRR sample which covers an area of 4.24 sr and has a source density of  $41 \text{ sr}^{-1}$ . The higher source density is mainly due to the difference in flux-density cutoff. The 3CRR sample is defined by  $S_{178} \geq 10.9 \text{ Jy}$ , based on the flux-density scale of Baars et al. (1977) which agrees (at 408 MHz) with that of Wyllie (1969a) to 3%. A source with  $S_{178} = 10.9 \text{ Jy}$  and spectral index of  $\alpha = -0.81$ , the median value for the 3CRR sample, will have  $S_{408} = 5.6 \text{ Jy}$ . The sky distribution of the MS4 sources is shown in Figure 1.

The higher selection frequency means that the MS4 sample will have slightly different properties from the 3CRR, containing more flat-spectrum sources. Because of the shape of the radio luminosity function, the lower flux-density cutoff means that the MS4 sample will contain a larger fraction of sources at high redshift.

## 3. OBSERVATIONS AT 843 MHz

The sources have all been imaged with the Molonglo Observatory Synthesis Telescope (MOST) at 843 MHz. With better resolution and sensitivity than the 408 MHz Molonglo

Cross, the MOST provides improved information about source positions, structures, and blends. Flux densities at 843 MHz conveniently bridge the gap between 408 and 1400 MHz. The positional accuracy of about  $1''$  available with MOST makes it possible to obtain unambiguous optical identifications for most strong sources, even when the optical counterpart is faint.

The MOST is described by Mills (1981), Robertson (1991), and references therein. It was constructed from the 1.6 km east-west arm of the 408 MHz Molonglo Cross Telescope, and modified to operate at 843 MHz with a bandwidth of 3 MHz. Rather than recording complex visibilities, the MOST forms a comb of 128 fan beams in real time. An image of the sky is reconstructed from the fan-beam responses using back-projection (Perley 1979). The synthesised beam is  $43'' \times 43'' \text{ cosec } |\delta|$ , and the basic field size is  $23' \times 23' \text{ cosec } |\delta|$ ; beam switching allows field sizes of up to  $160'$  to be observed (Bock et al. 1999). It requires twelve hours for full hour-angle coverage, in which case the  $uv$  plane is totally filled within an ellipse, apart from a small hole at the centre corresponding to the 15 m gap between the East and West arms.

### 3.1. ‘CUTS’ Observing

Because of the large number of sources, the observations were done in ‘CUTS’ mode, a method of time-sharing in which about ten sources are observed in one 12-hour session. Most of the CUTS observing was performed by R.W.H. in 1985 and 1986, as part of a program to establish a grid of calibrators for MOST (Campbell-Wilson & Hunstead 1994). Each source was observed in a cyclic schedule under computer control, with typical dwell times (CUTS) of 4 minutes at each of eight widely spaced hour angles. One or two unresolved sources were included as calibrators in each cycle.

In total 196 sources from the MS4 sample were observed in these CUTS runs, with the remainder being covered by full synthesis observations. Data reduction was performed using in-house software written by C. R. Subrahmanya, J. E. Reynolds, and T. Ye. The imaging process for CUTS is essentially the same as for full-synthesis data, but the software also allows calibration and viewing of individual CUTS, enabling angular sizes of compact sources to be estimated more accurately than from two-dimensional images.

### 3.2. Angular Sizes and Position Angles

The signal in each CUT consists of a one-dimensional projection of the sky brightness distribution, convolved with the telescope’s instantaneous point-spread function. Because they had higher angular resolution than the final two-dimensional images, the 1-D CUTS profiles were used to measure angular sizes and detect incipient double structure. The profiles were first deconvolved, using a 1-D CLEAN algorithm with a Gaussian restoring beam of FWHM  $30''$ . The dirty beam was estimated from the median of the CUTS profiles of the calibrators.

The largest angular extent and position angle of slightly resolved sources were determined by fitting a rectified sinewave to deconvolved source width as a function of hour angle. Comparison of repeat observations, and with higher-resolution ATCA images (Paper II), shows that for sources with  $\text{LAS} > 15''$ , the position angles were accurate to about  $5^\circ$ , and the angular sizes to about  $3''$ .

For sources resolved into doubles we fitted a Gaussian to each component and measured the component separation directly. For sources with  $\text{LAS} > 1'$  which were not edge-brightened doubles, we used the two-dimensional images to measure the angular size.

### 3.3. Imaging and Deconvolution

After removing individual CUTS affected by confusion in the fan beams, we formed raw two-dimensional images by back-projection. These images were then deconvolved with the standard CLEAN algorithm, using a dirty beam formed from the 1-D calibrator template. An example of raw and CLEANed CUTS images is shown in Hunstead (1991).

The dynamic range of the CLEANed images, defined as the ratio of the peak to the rms noise, was typically about 100:1, and was limited mainly by sidelobes from off-field sources, and by small variations in beam shape during the observation. For well resolved sources ( $\text{LAS} \gtrsim 3'$ ), the dynamic range was also limited by the success of CLEAN in modelling extended structure. The dynamic range, although lower than available from a full-synthesis observation, was sufficient to define structure on arcminute angular scales, and to provide reliable positions.

Figure 2 contains MOST CUTS images of a selection of 12 MS4 sources which appear extended at 843 MHz but which were not noted as extended in the MRC; all have angular extent  $< 2'$ .

### 3.4. Positions and Flux Densities

Peak and centroid positions, and peak and integrated flux densities were measured from the CLEANed images. The peak positions and flux densities were obtained using a biquadratic fit to the pixel of highest flux density and the four pixels surrounding it.

#### 3.4.1. Flux Densities

Integrated flux densities were obtained using the method of Jones (1989b). This involved considering the source brightness distribution as a surface in three-dimensional space, with the vertical axis proportional to flux density per beam area. The volume beneath this surface, and above a given base level, was plotted as a function of base level and then extrapolated to a base level of zero. A zero base level was used because there was no evidence of a negative bowl — the absolute value of the mean flux density in the area surrounding the sources was well below the rms noise.

The flux-density scale used is that of Calabretta (1985), which was based on interpolation between 408 MHz Molonglo and 2700 MHz Parkes flux densities. Comparison of this scale with that of Caganoff (1984), based on absolute flux-density measurements at 843 MHz, yielded a mean flux-density ratio of  $0.99 \pm 0.03$  for seven strong sources (Hunstead 1991). No northern hemisphere 843 MHz measurements are available for further comparisons. We estimate the external accuracy of the flux-density calibration to be about  $\pm 5\%$ . Based on repeated observations, we estimate the total flux-density error for compact sources ( $\text{LAS} \leq 1'$ ) to be  $\pm 7\%$  and for extended sources ( $\text{LAS} > 1'$ ) to be about  $\pm 10\%$ .

Comparison of integrated flux densities of 32 sources in the present study with the values reported by JM92 showed a significant systematic difference, with a mean ratio JM92/MS4 of  $0.94 \pm 0.02$ , with a standard deviation of 0.12. The difference was significant at the 2% level, using a two-tailed Wilcoxon signed-rank test on the fractional difference in flux density. While the cause of this difference is unclear, the CUTS-based flux densities were preferred because they were more consistent with adjacent points in the radio spectra.

#### 3.4.2. Positions

Position calibration of MOST is tied to a grid of unresolved sources ( $\text{LAS} < 10''$ ) with accurate centroid positions measured at 843 MHz (Hunstead 1991). The calibrator errors are estimated to be  $\sim 0.''2$  rms in right ascension and  $\sim 0.''2 \csc |\delta|$  rms in declination,

with systematic errors  $< 0''.1$  (Campbell-Wilson & Hunstead 1994).

We calculated the mean offsets in right ascension and declination for all the calibrators in each CUTS run, and used these to correct the measured target-source positions. The rms scatter was  $1''.0$  in  $\alpha$ , and  $1''.1 \cos \delta$  in  $\delta$ . We also tested positional accuracy by comparing positions of 16 target sources in repeated observations. Median differences between pairs of positions for the 12 sources with  $\text{LAS} < 1'.5$  were  $0''.5$  in RA and  $0''.9 \cos \delta$  in Dec, and for the four sources with  $\text{LAS} > 1'.5$ , the median differences were  $1''.5$  in RA and  $1''.9 \cos \delta$  in Dec. The error for extended sources is larger because of the uncertainties in determining the centroid at low flux-density levels.

The adopted position errors for the CUTS observations are therefore  $\Delta\alpha = 1''.0$ ,  $\Delta\delta = 1''.1 \cos \delta$  for sources with angular extent  $< 1'.5$ , and  $\Delta\alpha = 1''.5$ ,  $\Delta\delta = 1''.9 \cos \delta$  for sources with angular extent  $> 1'.5$ .

#### 4. ESTIMATION OF FLUX DENSITIES AT 178 MHz

To compare the properties of the MS4 sources with those in the northern 3CRR sample, flux densities at 178 MHz were estimated by interpolation or extrapolation from the radio spectrum. In Section 6, these flux densities will be used to define a southern 3CRR-equivalent sample.

For most sources the only flux-density measurements below 178 MHz were those from the 85.5 MHz survey of Mills, Slee, and Hill (Mills et al. 1960, 1961), and those at 80 and 160 MHz measured with the Culgoora radioheliograph (Slee & Higgins 1973, Slee & Higgins 1975 and Slee 1977; revised by Slee 1995). Because of their importance for interpolation, the 85.5 MHz MSH and 80 MHz Culgoora values were compared to look for any systematic differences. The Culgoora flux densities, measured with a  $3'.7$  beam, were expected to be low for some extended sources, while the MSH values, measured with a  $50'$  beam, were likely to be overestimated due to confusion. It was therefore expected that the MSH values would be higher on average. If anything, the plot in Figure 3 shows that the opposite is true, although the scatter is large. Since the plot does not indicate a clear preference, both 80 and 85.5 MHz values were used in the fit (if available), unless other information led us to prefer one of the values.

Interpolation or extrapolation was done by performing a weighted least-squares polynomial fit to  $\log S_\nu$  as a function of  $\log \nu$ . A quadratic fit was used in the first instance. If the reduced  $\chi^2$  for the fit was greater than 5, or if individual data points with small listed errors lay far from the fitted curve, a linear or cubic fit was attempted, depending on the apparent

curvature of the spectrum and on the number of data points. Anomalous data points were excluded from the fit if there was evidence of confusion or over-resolution, or if the source was known to be variable. As the object was to optimise the fit at 178 MHz, high-frequency points ( $\nu \geq 2700$  MHz) were more likely to be excluded if they did not fit well with the low frequency spectrum.

Our estimates of  $S_{178}$  are listed in Column 4 of Table 5; the order of the polynomial fit to  $\log \nu$  is given to the right of the flux density. Comments are given below for sources in which the fit may be unreliable, based either on a large  $\tilde{\chi}^2$  or on other information.

#### 4.1. Comments on Individual 178 MHz Estimates

**MRC B0008–421:** Required extrapolation below 408 MHz; estimated  $S_{178}$  is unreliable as the radio spectrum is curved.

**MRC B0240–422:** The value of  $S_{160} = 11.5$  Jy is higher than expected from the fit; if correct, this source should be included in our southern equivalent of the 3CRR sample (§ 6).

**MRC B0438–436:** Very compact source; the fit is probably affected by flux-density variability.

**MRC B0454–463:** Poor fit at low frequency ( $\tilde{\chi}^2 = 11.5$ ). A 5 GHz ATCA image (Paper 2) shows the radio structure to be core-dominated; the source is known to vary at high frequency (Wall et al. 1975; Wright et al. 1977).

**MRC B0511–484:** Most flux densities are affected by blending with two fainter sources;  $S_{178}$  relies on extrapolation below 408 MHz.

**MRC B0647–475:** Compact source with a curved spectrum and flux densities at only four frequencies.

**MRC B1315–460:** Compact source with a curved spectrum and flux densities at only four frequencies.

**PKS B1318–434:** Flux densities are affected by confusion from Centaurus A, making the extrapolation to 178 MHz unreliable. A quadratic fit to the four data points has been adopted; if the spectrum is really straight the source is probably stronger than the 3CRR cutoff of  $S_{178} = 10.9$  Jy.

**MRC B1445–468:** The measurements at 80 and 85.5 MHz are highly discrepant, so the fitted  $S_{178}$  is unreliable.

**MRC B1545–321:** Giant radio galaxy ( $\text{LAS} = 7'$ ). The estimate of  $S_{178}$  is unreliable as it relies on extrapolation from 843 MHz.

**MRC B1549–790:** Flat-spectrum source, known to vary at 843 MHz (Gaensler & Hunstead 2000);  $S_{178}$  relies on extrapolation and may be unreliable.

**MRC B1933–587:** Poor fit to a polynomial at low frequency. A 5 GHz ATCA image (Paper 2) shows the radio structure to be core-dominated; the source is known to vary at high frequency (Wall et al. 1975; Wright et al. 1977), but is non-variable at 843 MHz (Gaensler & Hunstead 2000).

**MRC B1934–638:**  $S_{178}$  for this GPS source is very uncertain. We used the cubic polynomial fitted by Reynolds (1994).

**MRC B2153–699:** Extrapolation unreliable because of blending with MRC B2152–699.

## 5. SUMMARY OF THE MS4 SAMPLE

A summary of the 843 MHz data for the MS4 sample, along with flux density measurements from the literature at other frequencies, is given in Table 5. Although different measurements in the literature have used (nominally) different flux-density scales, no correction has been made; the figures in the table are quoted *directly* from the papers cited. The columns of Table 5 are as follows:

1. Source name, taken from the MRC, unless the source has more than one MRC entry, in which case the name is from the original Parkes catalogue (Bolton et al. 1964; Price & Milne 1965) or Parkes 2700 MHz catalogue (Bolton et al. 1979 and references therein).
2. Right ascension in J2000 coordinates at 843 MHz.
3. Declination in J2000 coordinates at 843 MHz. The reference for the radio position in columns 2 and 3 is the same as for the 843 MHz flux density in column 7.
4. Estimated flux density at 178 MHz, as described in Section 4, and the order of the polynomial used to calculate the estimate.
5. Flux density at 80 MHz; the observing frequency is 85.5 MHz, if taken from MSH, or 80 MHz, if measured with the Culgoora Circular Array. The latter flux densities are from the compilation of Slee (1995), with revised calibration.



6. Flux density at 408 MHz, taken from the MRC, except for some extended sources. In general, flux densities were taken from published data in the following order of preference: SM75, MC4, Wyllie (1969b), the Parkes catalogues, Ekers et al. (1989). Flux densities for a few sources were estimated using the Molonglo Transit Catalogue or from the radio spectrum.
7. Flux density at 843 MHz, measured with MOST. The values of Campbell-Wilson & Hunstead (1994) were used for MOST calibrators, as were those of Subrahmanyan et al. (1996) for six giant radio sources. For the remaining sources the flux density was taken either from JM92 or from the present study, depending on which image had the higher dynamic range.
8. Flux density at 1400 MHz. Data are mostly from Parkes (1410 MHz: Bolton et al. 1964; Price & Milne 1965; Wills 1975), from Owens Valley (1425 MHz: Fomalont 1968; Fomalont & Moffet 1971), or from the NRAO VLA Sky Survey catalog (NVSS; 1400 MHz: Condon et al. 1998). For a few sources data were taken from the Instituto Argentino de Radioastronomia (IAR) 30 m telescope (1410 MHz: Quiniento et al. 1988; Quiniento & Echave 1990; Quiniento & Cersosimo 1993), from the Fleurs Synthesis Telescope, or the Australia Telescope Compact Array. The flux-density scale for the Parkes catalogues (Bolton et al. 1964; Price & Milne 1965) and Owens Valley data was that of Conway et al. (1963), whereas the data of Wills (1975) and the IAR 30 m data were on the scale of Wills (1973). At 1410 MHz the scale of Wills (1973) is 1.08 times the scale of Conway et al. (1963) (Baars et al. 1977). NVSS used the flux density scale of Baars et al. (1977).
9. Flux density at 2700 MHz, measured with the Parkes telescope, except for one source which was observed at 2640 MHz with Owens Valley (Rogstad & Ekers 1969). 2650 MHz flux densities are from the original Parkes catalogue or from Wills (1975), while 2700 MHz values are from the Parkes 2700 MHz survey or from Wills (1975). The Parkes 2700 MHz survey used a scale in which the peak flux density of Hydra A was 23.5 Jy; Wills (1975) used the flux-density scale of Wills (1973).
10. Flux density at 5000 MHz, measured with the Parkes telescope. Values at 4850 MHz are from the Parkes-MIT-NRAO survey (PMN: Gregory et al. 1994; Wright et al. 1996), those at 5000 MHz are from Wills (1975), and those at 5009 MHz are from Wills (1975), or the Parkes 2700 MHz survey, or Shimmins et al. (1969), or Shimmins & Bolton (1972a). The PMN survey used the flux density scale of Baars et al. (1977); Wills (1975) used the scale of Wills (1973); the Parkes 2700 MHz surveys used a 5 GHz scale in which the peak flux density of Hydra A was  $S_{5009} = 13.05$  Jy, as did Shimmins et al. (1969) and Shimmins & Bolton (1972a).

11. Radio spectral index  $\alpha$  measured between 408 and 2700 MHz, defined in the sense  $S_\nu \propto \nu^\alpha$ . For sources without measurements at both those frequencies, the spectral index was measured either between 408 and 5000 MHz or between 843 and 5000 MHz.
12. Largest angular size (LAS) at 843 MHz. The reference is the same as for the 843 MHz flux density, except for a few sources, noted in Section 5.1. We have imaged all sources with  $\text{LAS} < 35''$  with the ATCA at 5 GHz (Paper II), with the exception of MRC B0521–365, MRC B0743–673, MRC B1740–517, MRC B1814–519, MRC B2153–699, and MRC B2259–375.
13. Position angle of extension at 843 MHz, defined in degrees east of north (modulo 90). The reference is the same as for the 843 MHz flux density, except for a few sources which are noted in Section 5.1.

### 5.1. Comments on Individual Sources

**MRC B0208–512:** Detected with EGRET (Thompson et al. 1995).

**MRC B0214–480:** The Parkes 408 MHz and MSH 85.5 MHz flux densities are probably affected by blending with MRC B0211–479. The position, angular size, and position angle in Table 5 are from JM92, but  $S_{843}$  was measured from MOST images from the SUMSS survey (Mauch et al. 2003).

**MRC B0252–712:** The spectrum turns over at low frequency. The flux density of  $S_{85.5} = 7 \text{ Jy}$  is noted as uncertain in MSH, but corresponds well with the slight spectral curvature evident at higher frequencies.

**PKS B0319–45:** Giant radio galaxy. Because of the large angular size, the flux densities are uncertain. The MSH 85.5 MHz measurement was affected by sidelobes of Fornax A.

**MRC B0320–373:** Fornax A.

**MRC B0336–355:** Blended at low resolution with the foreground source MRC B0336–356. At 2650 and 5009 MHz, the peak flux densities (Wills 1975) were used, as they are expected to be less affected by blending.

**MRC B0411–346A:** The weaker source MRC B0411–346B is unrelated.

**MRC B0453–301, MRC B0456–301:** MSH 04–314 is a blend of these two sources.

**MRC B0506–612:** The 8.87 GHz flux density of 2.63 Jy (Shimmings & Wall 1973) is substantially higher than expected from the radio spectrum, probably indicating high-frequency

variability.

**MRC B0511–484:** Unequal double, with two neighbouring weaker sources, presumed to be unrelated. The SM75 integrated value of  $S_{408} = 8.8$  Jy is affected by blending. The MRC fitted value of 6.84 Jy was preferred but is still uncertain. The Parkes flux densities at 2.7 and 5 GHz are also affected by blending, so the radio spectrum is not well determined.

**MRC B0518–458:** Pictor A.

**MRC B0521–365:** Well studied blazar, detected as a gamma-ray source by EGRET (Thompson et al. 1995).

**PKS B0707–35:** The flux density  $S_{5000} = 0.84$  Jy (Wall & Schilizzi 1979) appears anomalously high.

**MRC B0743–673:** The 1410 MHz flux density (Price & Milne 1965) is higher than expected from the radio spectrum, and probably affected by blending with MRC B0742–674.

**MRC B1017–421, MRC B1017–426:** MSH 10–44 is a blend of these two sources.

**MRC B1136–320:** In the Texas catalog (Douglas et al. 1996) the double separation is quoted as  $58''$  in P.A.  $-15^\circ$ , consistent with the values in Table 5.

**MRC B1143–316:** The Texas catalog (Douglas et al. 1996) lists this source as a double with separation  $34''$  in P.A.  $86^\circ$ . The MRC value of  $S_{408} = 5.77$  Jy is preferred to SM75’s anomalously low value of 3.8 Jy.

**MRC B1302–491:** Nearby edge-on spiral galaxy NGC 4945, identified by Mills et al. (1960).

**PKS B1318–434:** Complex double source, with bent edge-darkened lobes, lying behind the southern lobe of Centaurus A (Cooper et al. 1965; Haynes et al. 1983).

**MRC B1322–427:** The well studied low-luminosity radio galaxy Centaurus A (see review by Ebner & Balick 1983). The flux density at 843 MHz was determined from the radio spectrum.

**PKS B1400–33:** The only source in the sample which is not in the MRC. An unusual extended source of low surface brightness. There is a nearby compact source associated with the E0 galaxy NGC 5419 (see Ekers et al. 1989). Goss et al. (1987) suggest that the extended component may be a relic radio source associated with the poor cluster Abell S753 around NGC 5419. The radio properties have been studied in detail by Subrahmanyan et al. (2003); we have used their flux densities at 843 and 1398 MHz.

**MRC B1425–479:** Because of the angular size of  $4'.5$ , the values of  $S_{408}$  and  $S_{5000}$  in Table 5 may be slightly underestimated.

**MRC B1445–468:** The published values of  $S_{80} = 2$  Jy (Slee 1995) and 13 Jy (Slee & Higgins 1973) — are grossly discrepant. We prefer the latter value, after multiplying it by 1.1 to correct the flux-density scale (Slee 1977).

**MRC B1549–790:** Flat-spectrum source. The flux density at 1410 MHz (Price & Milne 1965) is affected by blending with MRC B1547–795.

**MRC B1814–637, MRC B1817–640:** MSH 18–61 is a blend of these two sources.

**MRC B1917–546:** Ultra-steep spectrum source. The 1410 MHz flux density may be affected by blending with two weak neighbouring sources (Hunstead 1972).

**MRC B1934–638:** Archetypal Gigahertz-Peaked-Spectrum (GPS) source (Bolton et al. 1963).

**MRC B1940–406:** Blending with three weaker sources (JM92) makes the radio spectrum uncertain.

**MRC B2006–566:** Very extended, diffuse source, associated with the cluster Abell 3667 (Abell et al. 1989). The flux density of  $S_{843} = (5.5 \pm 0.5)$  Jy (Röttgering et al. 1997) was obtained from a MOST full-synthesis image after subtracting the contribution from background sources within the source envelope (0.6 Jy); the discrepancy with JM92 is probably due to the higher noise level in their image.

**MRC B2052–474:** Detected with EGRET (Thompson et al. 1995).

**MRC B2122–555:** The MRC position appears to be in error, lying  $30''$  east of the MOST position. The MRC flux density of 4.05 Jy is also lower than expected from the radio spectrum, suggesting that the observation may have been affected by a large ionospheric wedge (Hunstead 1972). Both Parkes positions (Wall et al. 1975; Gregory et al. 1994) agree with the MOST centroid.

**MRC B2152–699:** Some flux densities are affected by blending with MRC B2153–699. The 1415 MHz measurement (Christiansen et al. 1977) was made with the Fleurs Synthesis Telescope. At 2650 MHz, the peak flux density (Wills 1975) was used, to reduce any contribution from MRC B2153–699.

**MRC B2153–699:** Double, extended along a position angle similar to that of MRC B2152–699. Flux densities are affected by blending with MRC B2152–699: both the MRC value of  $20.9 \pm 1.4$  Jy and the SM75 value of  $6.0 \pm 0.4$  Jy are regarded as unreliable. Therefore, the

flux densities at 843 and 1415 MHz, together with the 468 MHz value of  $10.7 \pm 0.9$  Jy (Ekers 1969b), have been used to estimate the flux density at 408 MHz.

## 6. DISCUSSION

The 178 MHz flux densities estimated in Section 4 have been used to define a strong source subsample of MS4 which we call SMS4. It has been chosen to have the same flux-density cutoff, 10.9 Jy, as the northern 3CRR sample, and contains 137 sources, compared with 172 in 3CRR.

Comparison of SMS4 with 3CRR (Table 6) shows the southern sample to have a slightly higher source density, but only at the  $2.8\sigma$  level of significance. The difference should be treated with caution and may simply reflect biases in the way each sample was compiled. We have identified three possible causes of such a bias:

- (i) As the spectra of many radio sources turn over at low radio frequency, extrapolation from high frequencies is more likely to overestimate than underestimate  $S_{178}$ . The survey with the Mauritius radio telescope (Golap et al. 1998) at 151.5 MHz will be valuable for checking flux densities of sources north of  $\delta = -70^\circ$ , and testing for such a bias in the SMS4 sample.
- (ii) Because of the steep slope of the radio source counts, a small systematic difference in flux-density scale can strongly bias the source density. The Mauritius values will be useful for checking such effects in SMS4.
- (iii) The 3CRR may be missing sources of low surface brightness. The angular size distributions are compared in Figure 4. The median angular size of SMS4 is  $32^{+6}_{-5}$  arcsec, compared with  $35.5^{+8.7}_{-7.5}$  arcsec for 3CRR. Although the medians are similar, the distributions appear different: the SMS4 has proportionally more sources with angular size  $> 300''$ , and proportionally fewer sources with angular size between  $100''$  and  $300''$ . However, because of the small numbers of sources involved, it is not possible to draw firm conclusions about differences in the angular size distributions.

The median flux density of SMS4 ( $S_{178} = 15.7$  Jy), is consistent with the median value of 15.6 Jy for 3CRR. This is to be expected if the radio source counts are similar. Histograms of spectral indices for the MS4, SMS4, and 3CRR samples are plotted in Figure 5. The distributions for the MS4 sample show a longer tail towards flatter spectral indices than do those of the SMS4 or 3CRR. This is to be expected given the higher selection frequency

of the MS4, as flat-spectrum sources will be included which would be missed with a higher flux-density cutoff and lower selection frequency. The median spectral indices,  $\alpha = -0.91$  for SMS4 and  $-0.81$  for 3CRR (Table 6), are not consistent, but can be explained simply by the different frequency ranges used to measure  $\alpha$  for each sample: 408–2700 MHz for SMS4 and 178–750 MHz for 3CRR. Given that the spectra of many radio sources turn over at low frequency, and that radio spectra often steepen at high frequency, the flatter median spectral index of the 3CRR sources can be explained by the lower frequency range over which  $\alpha$  was measured. A comparison over more similar frequency ranges will be possible when 151.5 MHz data from Mauritius become available.

## 7. SUMMARY

The Molonglo Southern 4 Jy (MS4) sample, a complete sample of radio sources south of  $\delta = -30^\circ$ , has been selected from the Molonglo Reference Catalogue (MRC) to have  $S_{408} > 4.0$  Jy. All the MS4 sources have been imaged with MOST at 843 MHz, thus providing more accurate positions than available from the MRC. The positional accuracy is about  $\Delta\alpha = 1''.0$ ,  $\Delta\delta = 1''.1 \operatorname{cosec} |\delta|$  for compact sources (angular size  $< 1'.5$ ), and  $\Delta\alpha = 1''.5$ ,  $\Delta\delta = 1''.9 \operatorname{cosec} |\delta|$  for extended sources (angular size  $> 1'.5$ ). Integrated flux densities at 843 MHz have been measured from the images, and have an accuracy of  $\sim 7$ –10%. Reliable angular sizes and position angles have been measured for sources with angular extent  $\gtrsim 15''$ . The median angular size for the MS4 sample as measured with MOST is  $23'' \pm 4''$ .

The set of MOST images provides a useful database for optical identification, as well as for planning higher-resolution radio imaging, to be presented in Paper II. Radio flux densities at other frequencies have been obtained from the literature, and used to retrospectively define a stronger subsample, the SMS4, with the same flux-density limit as the 178 MHz 3CRR sample. Preliminary comparisons of SMS4 and 3CRR show that their overall properties are similar.

## ACKNOWLEDGEMENTS

We thank staff and students of the School of Physics, University of Sydney, for their generous help with observing and data reduction. Special thanks to the staff of the Molonglo Telescope, for operating and maintaining it for the demanding CUTS runs, and to T. Ye and C. R. Subrahmanya for writing and modifying data-reduction software.

We have made use of NASA’s Astrophysics Data System Abstract Service, and the

NASA/IPAC Extragalactic Database (NED) which is operated by the Jet Propulsion Laboratory, Caltech, under contract with the US National Aeronautics and Space Administration. The Molonglo Observatory Synthesis Telescope is funded by both the Australian Research Council and the Science Foundation for Physics within the University of Sydney. AMB acknowledges the receipt of an Australian Postgraduate Research Award over the period of this research.

## REFERENCES

- Abell, G. O., Corwin, H. G., & Olowin, R. P. 1989, *ApJS*, 70, 1
- Alvarez, H., Aparici, J., May, J., & Reich, P. 2000, *A&A*, 355, 863
- Baars, J. W. M., Genzel, R., Pauliny-Toth, I. I. K., & Witzel, A. 1977, *A&A*, 61, 99
- Bennett, A. S. 1962, *Mem. R. Astron. Soc.*, 68, 163
- Best, P. N., Röttgering, H. J. A., & Lehnert, M. D. 1999, *MNRAS*, 310, 223, [arXiv:astro-ph/9903471](#) (BRL99)
- Birkinshaw, M., Worrall, D. M., & Hardcastle, M. J. 2002, *MNRAS*, 335, 142, [arXiv:astro-ph/0204509](#)
- Bock, D. C.-J., Large, M. I., & Sadler, E. M. 1999, *AJ*, 117, 1578, [arXiv:astro-ph/9812083](#)
- Bolton, J. G. & Butler, P. W. 1975, *Aust. J. Phys. Astrophys. Suppl.*, 34, 33
- Bolton, J. G. & Clark, B. G. 1960, *PASP*, 72, 29
- Bolton, J. G., Gardner, F. F., & Mackey, M. B. 1963, *Nature*, 199, 682
- . 1964, *Aust. J. Phys.*, 17, 340
- Bolton, J. G. & Shimmins, A. J. 1973, *Aust. J. Phys. Astrophys. Suppl.*, 30, 1
- Bolton, J. G., Wright, A. E., & Savage, A. 1979, *Aust. J. Phys. Astrophys. Suppl.*, 46, 1
- Bosma, A., Goss, W. M., & Wellington, K. J. 1983, *A&AS*, 54, 387
- Burgess, A. M. & Hunstead, R. W. 2006, *AJ*, in press (Paper II)
- Burns, J. O., Feigelson, E. D., & Schreier, E. J. 1983, *ApJ*, 273, 128
- Caganoff, S. 1984, *Physics IV Honours Report*, University of Sydney
- Calabretta, M. R. 1985, *PhD thesis*, University of Sydney
- Cameron, M. J. 1971, *MNRAS*, 152, 439
- Campbell-Wilson, D. & Hunstead, R. W. 1994, *Proc. Astron. Soc. Aust.*, 11, 33
- Carter, D. & Malin, D. F. 1983, *MNRAS*, 203, 49P
- Chartas et al. 2000, *ApJ*, 542, 655, [arXiv:astro-ph/0005227](#)



- Choi, Y., Reynolds, C. S., Heinz, S., Rosenberg, J. L., Perlman, E. S., & Yang, J. 2004, *ApJ*, 606, 185, arXiv:astro-ph/0402131
- Christiansen, W. N., Frater, R. H., Watkinson, A., O’Sullivan, J. D., Lockhart, I. A., & Goss, W. M. 1977, *MNRAS*, 181, 183
- Clark et al. 1997, *MNRAS*, 286, 558
- Clarke, D. A., Burns, J. O., & Norman, M. L. 1992, *ApJ*, 395, 444
- Clarke, J. N., Little, A. G., & Mills, B. Y. 1976, *Aust. J. Phys. Astrophys. Suppl.*, 40, 1 (MC4)
- Combi, J. A. & Romero, G. E. 1997, *A&AS*, 121, 11
- Condon, J. J., Cotton, W. D., Greisen, E. W., Yin, Q. F., Perley, R. A., Taylor, G. B., & Broderick, J. J. 1998, *AJ*, 115, 1693
- Condon, J. J., Helou, G., Sanders, D. B., & Soifer, B. T. 1996, *ApJS*, 103, 81
- Conway, R. G., Kellermann, K. I., & Long, R. J. 1963, *MNRAS*, 125, 261
- Cooper, B. F. C., Price, R. M., & Cole, D. J. 1965, *Aust. J. Phys.*, 18, 589
- Dahlem, M., Golla, G., Whiteoak, J. B., Wielebinski, R., Huttemeister, S., & Henkel, C. 1993, *A&A*, 270, 29
- Danziger, I. J. & Goss, W. M. 1983, *MNRAS*, 202, 703
- Day, G. A., Shimmins, A. J., Ekers, R. D., & Cole, D. J. 1966, *Aust. J. Phys.*, 19, 35
- De Breuck, C., Hunstead, R. W., Sadler, E. M., Rocca-Volmerange, B., & Klammer, I. 2004, *MNRAS*, 347, 837, arXiv:astro-ph/0309814
- De Breuck, C., van Breugel, W., Röttgering, H. J. A., & Miley, G. 2000, *A&AS*, 143, 303, arXiv:astro-ph/0002297
- de Pater, I., Schloerb, F. P., & Johnson, A. H. 1985, *AJ*, 90, 846
- Dennison, B., Broderick, J. J., Ledden, J. E., & O’Dell, S. L. 1981, *AJ*, 86, 1604
- Douglas, J. N., Bash, F. N., Bozayan, F. A., Torrence, G. W., & Wolfe, C. 1996, *AJ*, 111, 1945
- Drinkwater et al. 1997, *MNRAS*, 284, 85, arXiv:astro-ph/9609019

- Duncan, R. A. & Sproats, L. N. 1992, *Proc. Astron. Soc. Aust.*, 10, 16
- Ebner, K. & Balick, B. 1983, *PASP*, 95, 675
- Edge, D. O., Shakeshaft, J. R., McAdam, W. B., Baldwin, J. E., & Archer, S. 1959, *Mem. R. Astron. Soc.*, 68, 37
- Ekers, J. A. 1969a, *Aust. J. Phys. Astrophys. Suppl.*, 7, 1
- Ekers, R. D. 1969b, *Aust. J. Phys. Astrophys. Suppl.*, 6, 1
- Ekers, R. D., Goss, W. M., Kotanyi, C. G., & Skellern, D. J. 1978, *A&A*, 69, L21
- Ekers, R. D., Goss, W. M., Wellington, K. J., Bosma, A., Smith, R. M., & Schweizer, F. 1983, *A&A*, 127, 361
- Ekers, R. D. & Whiteoak, J. B. 1992, *Journal of Electrical and Electronics Engineering, Australia*, 12, 225
- Ekers et al. 1989, *MNRAS*, 236, 737
- Elmouttie, M., Haynes, R. F., Jones, K. L., Ehle, M., Beck, R., Harnett, J. I., & Wielebinski, R. 1997, *MNRAS*, 284, 830
- Fomalont, E. B. 1968, *ApJS*, 15, 203
- Fomalont, E. B., Ebner, K. A., van Breugel, W. J. M., & Ekers, R. D. 1989, *ApJ*, 346, L17
- Fomalont, E. B. & Moffet, A. T. 1971, *AJ*, 76, 5
- Forbes, D. A. & Norris, R. P. 1998, *MNRAS*, 300, 757, [arXiv:astro-ph/9804298](#)
- Fosbury, R. A. E., Morganti, R., Wilson, W., Ekers, R. D., di Serego Alighieri, S., & Tadhunter, C. N. 1998, *MNRAS*, 296, 701, [arXiv:astro-ph/9801249](#)
- Fosbury et al. 1982, *MNRAS*, 201, 991
- Gaensler, B. M. & Hunstead, R. W. 2000, *Publ. Astron. Soc. Aust.*, 17, 72, [arXiv:astro-ph/9911194](#)
- Gardner, F. F. & Whiteoak, J. B. 1971, *Aust. J. Phys.*, 24, 899
- Gardner, F. F., Whiteoak, J. B., & Morris, D. 1969, *Aust. J. Phys.*, 22, 821
- Geldzahler, B. J. & Fomalont, E. B. 1984, *AJ*, 89, 1650

- Glozzi, M., Brinkmann, W., Laurent-Muehleisen, S. A., Takalo, L. O., & Sillanpää, A. 1999, *A&A*, 352, 437, arXiv:astro-ph/9911055
- Golap, K., Udaya Shankar, N., Sachdev, S., Dodson, R., & Sastry, C. V. 1998, *JA&A*, 19, 35, arXiv:astro-ph/9808062
- Goldstein, S. J. 1962, *AJ*, 67, 171
- Goss, W. M., Ekers, R. D., Skellern, D. J., & Smith, R. M. 1982, *MNRAS*, 198, 259
- Goss, W. M., McAdam, W. B., Wellington, K. J., & Ekers, R. D. 1987, *MNRAS*, 226, 979
- Gregorini, L., de Ruiter, H. R., Parma, P., Sadler, E. M., Vettolani, G., & Ekers, R. D. 1994, *A&AS*, 106, 1
- Gregory, P. C., Vavasour, J. D., Scott, W. K., & Condon, J. J. 1994, *ApJS*, 90, 173
- Griffith, M. R., Wright, A. E., Burke, B. F., & Ekers, R. D. 1994, *ApJS*, 90, 179
- . 1995, *ApJS*, 97, 347
- Haigh, A. D. 2000, PhD thesis, University of Sydney
- Hardcastle, M. J., Worrall, D. M., & Birkinshaw, M. 1999, *MNRAS*, 305, 246, arXiv:astro-ph/9812148
- Hardcastle, M. J., Worrall, D. M., Kraft, R. P., Forman, W. R., Jones, C., & Murray, S. S. 2003, *ApJ*, 593, 169, arXiv:astro-ph/0304443
- Harnett, J. I. 1987, *MNRAS*, 227, 887
- Harnett, J. I., Haynes, R. F., Klein, U., & Wielebinski, R. 1989, *A&A*, 216, 39
- Harnett, J. I., Haynes, R. F., Wielebinski, R., & Klein, U. 1990, *Proc. Astron. Soc. Aust.*, 8, 257
- Harnett, J. I. & Reynolds, J. E. 1985, *MNRAS*, 215, 247
- Haslam et al. 1981, *A&A*, 100, 209
- Haynes, R. F., Cannon, R. D., & Ekers, R. D. 1983, *Proc. Astron. Soc. Aust.*, 5, 241
- Heeschen, D. S. 1961, *ApJ*, 133, 322
- Heinz, S., Choi, Y., Reynolds, C. S., & Begelman, M. C. 2002, *ApJ*, 569, L79, arXiv:astro-ph/0201107

- Hunstead, R. W. 1972, MNRAS, 157, 367
- . 1991, Aust. J. Phys., 44, 743
- Hunstead, R. W., Durdin, J. M., Little, A. G., Reynolds, J. E., & Kesteven, M. J. 1982, Proc. Astron. Soc. Aust., 4, 447
- Jauncey, D. L. 1968, ApJ, 152, 647
- Jones, P. A. 1989a, Proc. Astron. Soc. Aust., 8, 81
- . 1989b, PhD thesis, University of Sydney
- . 1992, Aust. J. Phys., 45, 797
- Jones, P. A. & McAdam, W. B. 1992, ApJS, 80, 137 (JM92)
- Junkes, N., Haynes, R. F., Harnett, J. I., & Jauncey, D. L. 1993a, A&A, 269, 29
- . 1993b, A&A, 274, 1009
- Kaufmann, P., Scalise, E., Marques dos Santos, P., & Fogarty, W. G. 1974, MNRAS, 169, 15P
- Keel, W. C. 1986, ApJ, 302, 296
- Killeen, N. E., Bicknell, G. V., & Ekers, R. D. 1986, ApJ, 302, 306
- Killeen, N. E. B. & Bicknell, G. V. 1988, ApJ, 325, 180
- Kraft, R. P., Forman, W. R., Jones, C., Murray, S. S., Hardcastle, M. J., & Worrall, D. M. 2002, ApJ, 569, 54, arXiv:astro-ph/0111340
- Kraft et al. 2003, ApJ, 592, 129, arXiv:astro-ph/0304363
- Laing, R. A., Riley, J. M., & Longair, M. S. 1983, MNRAS, 204, 151
- Large, M. I., Mills, B. Y., Little, A. G., Crawford, D. F., & Sutton, J. M. 1981, MNRAS, 194, 693
- Lloyd, B. D. & Jones, P. A. 2002, MNRAS, 331, 717
- Lloyd, B. D., Jones, P. A., & Haynes, R. F. 1996, MNRAS, 279, 1197
- Lockhart, I. A. & Sheridan, K. V. 1970, Proc. Astron. Soc. Aust., 1, 344

- Mantovani, F. 1982, *A&A*, 110, 345
- Mantovani, F., Junor, W., Fanti, R., Padrielli, L., Browne, I. W. A., & Muxlow, T. W. B. 1992, *MNRAS*, 257, 353
- Marvel, K. B., Shukla, H., & Rhee, G. 1999, *ApJS*, 120, 147
- Mauch et al. 2003, *MNRAS*, 342, 1117
- McAdam, W. B. & Schilizzi, R. T. 1977, *A&A*, 55, 67
- McAdam, W. B., White, G. L., & Bunton, J. D. 1988, *MNRAS*, 235, 425
- McGee, R. X., Slee, O. B., & Stanley, G. J. 1955, *Aust. J. Phys.*, 8, 347
- Meisenheimer, K., Röser, H.-J., Hiltner, P. R., Yates, M. G., Longair, M. S., Chini, R., & Perley, R. A. 1989, *A&A*, 219, 63
- Mills, B. Y. 1981, *Proc. Astron. Soc. Aust.*, 4, 156
- Mills, B. Y., Aitchison, R. E., Little, A. G., & McAdam, W. B. 1963, *Proc. Inst. Radio Engrs. Aust.*, 24, 156
- Mills, B. Y., Slee, O. B., & Hill, E. R. 1958, *Aust. J. Phys.*, 11, 360
- . 1960, *Aust. J. Phys.*, 13, 676
- . 1961, *Aust. J. Phys.*, 14, 497
- Morganti, R., Killeen, N. E. B., Ekers, R. D., & Oosterloo, T. A. 1999a, *MNRAS*, 307, 750, [arXiv:astro-ph/9903448](#)
- Morganti, R., Killeen, N. E. B., & Tadhunter, C. N. 1993, *MNRAS*, 263, 1023
- Morganti, R., Oosterloo, T., Tadhunter, C. N., Aiudi, R., Jones, P., & Villar-Martin, M. 1999b, *A&AS*, 140, 355, [arXiv:astro-ph/9910150](#)
- Morganti, R., Oosterloo, T. A., Tadhunter, C. N., van Moorsel, G., Killeen, N., & Wills, K. A. 2001, *MNRAS*, 323, 331, [arXiv:astro-ph/0010636](#)
- Norris et al. 1990, *Proc. Astron. Soc. Aust.*, 8, 252
- O’Dea, C. P., Baum, S. A., Maloney, P. R., Tacconi, L. J., & Sparks, W. B. 1994, *ApJ*, 422, 467

- Otani, C., Brinkmann, W., Böhringer, H., Reid, A., & Siebert, J. 1998, *A&A*, 339, 693
- Otrupcek, R. E. & Wright, A. E. 1991, *Proc. Astron. Soc. Aust.*, 9, 170
- Ott, M., Whiteoak, J. B., Henkel, C., & Wielebinski, R. 2001, *A&A*, 372, 463, arXiv:astro-ph/0109190
- Parma, P., Cameron, R. A., & Deruitter, H. R. 1991, *AJ*, 102, 1960
- Perley, R. A. 1979, *AJ*, 84, 1443
- Perley, R. A., Röser, H.-J., & Meisenheimer, K. 1997, *A&A*, 328, 12
- Price, R. M. & Milne, D. K. 1965, *Aust. J. Phys.*, 18, 329
- Quiniento, Z. M. & Cersosimo, J. C. 1993, *A&AS*, 97, 435
- Quiniento, Z. M., Cersosimo, J. C., & Colomb, F. R. 1988, *A&AS*, 76, 21
- Quiniento, Z. M. & Echave, M. M. 1990, *A&AS*, 83, 393
- Rayner, D. P., Norris, R. P., & Sault, R. J. 2000, *MNRAS*, 319, 484
- Reid, R. I., Kronberg, P. P., & Perley, R. A. 1999, *ApJS*, 124, 285
- Reynolds, J. 1994, Flux Scale for the AT Compact Array, Tech. Rep. 39.3/040, ATNF
- Reynolds et al. 1993, in *Sub-arcsecond Radio Astronomy*, ed. R. J. Davis & R. S. Booth (Cambridge: Cambridge University Press), 156
- Robertson, J. G. 1991, *Aust. J. Phys.*, 44, 729
- Robertson, J. G. & Smith, R. M. 1981, *Proc. Astron. Soc. Aust.*, 4, 187
- Rogstad, D. H. & Ekers, R. D. 1969, *ApJ*, 157, 481
- Röttgering, H. J. A., Wieringa, M. H., Hunstead, R. W., & Ekers, R. D. 1997, *MNRAS*, 290, 577
- Sadler, E. M. 1987, in *Observational Evidence of Activity in Galaxies*, ed. E. Y. Khachikian, K. J. Fricke, & J. Melnick, *IAU Symp.* 121 (Dordrecht: Reidel), 443
- Sadler, E. M. 1997, in *ASP Conf. Ser.*, Vol. 116, *The Second Stromlo Symposium: The Nature of Elliptical Galaxies*, ed. M. Arnaboldi, G. S. Da Costa, & P. Saha (San Francisco: ASP), 411

- Safouris, V., Hunstead, R. W., & Prouton, O. R. 2003, *Publ. Astron. Soc. Aust.*, 20, 1
- Saripalli, L., Subrahmanyam, R., & Hunstead, R. W. 1994, *MNRAS*, 269, 37
- Saripalli, L., Subrahmanyam, R., & Udaya Shankar, N. 2002, *ApJ*, 565, 256, [arXiv:astro-ph/0209570](#)
- . 2003, *ApJ*, 590, 181, [arXiv:astro-ph/0303157](#)
- Sarma, A. P., Troland, T. H., & Rupen, M. P. 2002, *ApJ*, 564, 696
- Sault, R. J. & Wieringa, M. H. 1994, *A&AS*, 108, 585
- Schilizzi, R. T. & McAdam, W. B. 1975, *Mem. R. Astron. Soc.*, 79, 1 (SM75)
- Schiminovich, D., van Gorkom, J. H., van der Hulst, J. M., & Kasow, S. 1994, *ApJ*, 423, L101
- Schreier, E. J., Burns, J. O., & Feigelson, E. D. 1981, *ApJ*, 251, 523
- Schwartz, D. A., Bradt, H. V., Remillard, R. A., & Tuohy, I. R. 1991, *ApJ*, 376, 424
- Schwartz et al. 2000, *ApJ*, 540, L69, [arXiv:astro-ph/0005255](#)
- Schwarz, U. J., Cole, D. J., & Morris, D. 1973, *Aust. J. Phys.*, 26, 661
- Schwarz, U. J., Whiteoak, J. B., & Cole, D. J. 1974, *Aust. J. Phys.*, 27, 563
- Shain, C. A. 1958, *Aust. J. Phys.*, 11, 517
- Sheridan, K. V. 1958, *Aust. J. Phys.*, 11, 400
- Shimmins, A. J. 1971, *Aust. J. Phys. Astrophys. Suppl.*, 21, 1
- Shimmins, A. J. & Bolton, J. G. 1972a, *Aust. J. Phys. Astrophys. Suppl.*, 23, 1
- . 1972b, *Aust. J. Phys. Astrophys. Suppl.*, 26, 1
- . 1974, *Aust. J. Phys. Astrophys. Suppl.*, 32, 1
- Shimmins, A. J. & Day, G. A. 1968, *Aust. J. Phys.*, 21, 377
- Shimmins, A. J., Day, G. A., Ekers, R. D., & Cole, D. J. 1966, *Aust. J. Phys.*, 19, 837
- Shimmins, A. J., Manchester, R. N., & Harris, B. J. 1969, *Aust. J. Phys. Astrophys. Suppl.*, 8, 1

- Shimmins, A. J. & Wall, J. V. 1973, *Aust. J. Phys. Astrophys. Suppl.*, 26, 93
- Simkin, S. M., Sadler, E. M., Sault, R., Tingay, S. J., & Callcut, J. 1999, *ApJS*, 123, 447, arXiv:astro-ph/9903313
- Slee, O. B. 1977, *Aust. J. Phys. Astrophys. Suppl.*, 43, 1
- . 1995, *Aust. J. Phys.*, 48, 143
- Slee, O. B. & Higgins, C. S. 1973, *Aust. J. Phys. Astrophys. Suppl.*, 27, 1
- . 1975, *Aust. J. Phys. Astrophys. Suppl.*, 36, 1
- Slee, O. B. & Sheridan, K. K. 1975, *Proc. Astron. Soc. Aust.*, 2, 336
- Slee, O. B., Sheridan, K. V., Dulk, G. A., & Little, A. G. 1983, *Proc. Astron. Soc. Aust.*, 5, 247
- Smith, R. M. 1983, PhD thesis, Australian National University
- Smith, R. M. & Bicknell, G. V. 1983, *Proc. Astron. Soc. Aust.*, 5, 251
- . 1986, *ApJ*, 308, 36
- Stephenson, F., Clark, D. H., & Crawford, D. F. 1977, *MNRAS*, 180, 567
- Subrahmanyan, R., Beasley, A. J., Goss, W. M., Golap, K., & Hunstead, R. W. 2003, *AJ*, 125, 1095, arXiv:astro-ph/0212154
- Subrahmanyan, R., Saripalli, L., & Hunstead, R. W. 1996, *MNRAS*, 279, 257
- Swarup, G. 1984, *JA&A*, 5, 139
- Tadhunter et al. 1988, *MNRAS*, 235, 403
- Tateyama, C. E. & Strauss, F. M. 1992, *MNRAS*, 256, 8
- Taylor, G. B., Barton, E. J., & Ge, J. P. 1994, *AJ*, 107, 1942
- Taylor, G. B., Fabian, A. C., & Allen, S. W. 2002, *MNRAS*, 334, 769, arXiv:astro-ph/0109337
- Thompson et al. 1995, *ApJS*, 101, 259
- Tingay et al. 1998, *ApJ*, 497, 594



- Turtle, A. J. & Amy, S. W. 1991, in *The Magellanic Clouds*, ed. R. Haynes & D. Milne, IAU Symp. 148 (Dordrecht: Kluwer), 114
- Ulvestad, J., Johnston, K., Perley, R., & Fomalont, E. 1981, *AJ*, 86, 1010
- Unewisse, A. M. 1993, PhD thesis, University of Sydney
- Van Gorkom, J. H., van der Hulst, J. M., Haschick, A. D., & Tubbs, A. D. 1990, *AJ*, 99, 1781
- Villar-Martín, M., Tadhunter, C., Morganti, R., Clark, N., Killeen, N., & Axon, D. 1998, *A&A*, 332, 479
- Wall, J. V. & Cole, D. J. 1973, *Aust. J. Phys.*, 26, 881
- Wall, J. V. & Schilizzi, R. T. 1979, *MNRAS*, 189, 593
- Wall, J. V., Shimmins, A. J., & Bolton, J. G. 1975, *Aust. J. Phys. Astrophys. Suppl.*, 34, 55
- Wardle, J. F., Moore, R. L., & Angel, J. R. P. 1984, *ApJ*, 279, 93
- White, G. L., McAdam, W. B., & Jones, I. G. 1984, *Proc. Astron. Soc. Aust.*, 5, 507
- Whiteoak, J. B. & Bunton, J. D. 1985, *Proc. Astron. Soc. Aust.*, 6, 171
- Whiteoak, J. B. & Gardner, F. F. 1968, *ApJ*, 154, 807
- Whiteoak, J. B. & Wilson, W. E. 1990, *MNRAS*, 245, 665
- Wills, B. J. 1973, *ApJ*, 180, 335
- . 1975, *Aust. J. Phys. Astrophys. Suppl.*, 38, 1
- Wright, A. E., Griffith, M. R., Burke, B. F., & Ekers, R. D. 1994, *ApJS*, 91, 111
- Wright, A. E., Griffith, M. R., Hunt, A. J., Troup, E., Burke, B. F., & Ekers, R. D. 1996, *ApJS*, 103, 145
- Wright, A. E., Savage, A., & Bolton, J. G. 1977, *Aust. J. Phys. Astrophys. Suppl.*, 41, 1
- Wyllie, D. V. 1969a, *MNRAS*, 142, 229
- . 1969b, *Proc. Astron. Soc. Aust.*, 1, 234

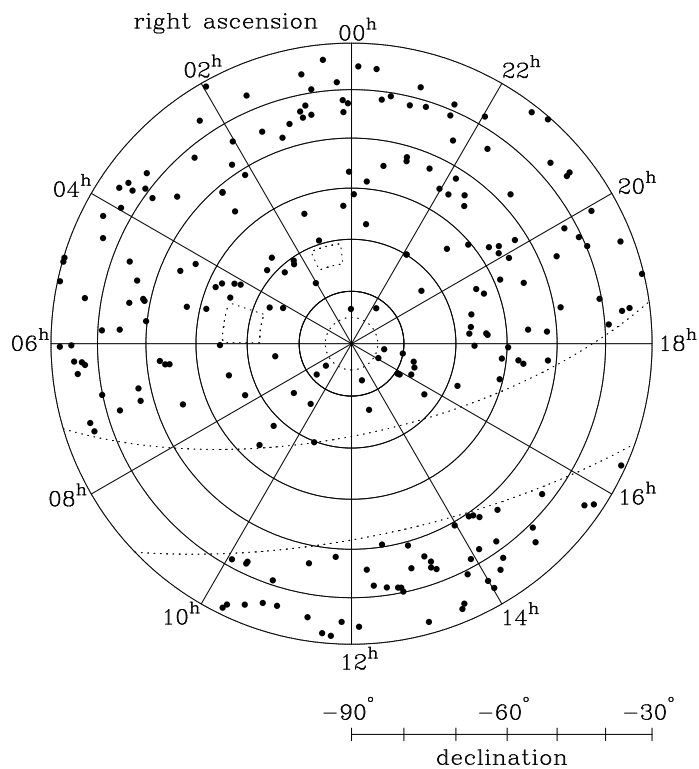


Fig. 1.— Plot of the source locations on a Lambert equal-area projection of the sky. The South Celestial Pole is at the centre of the plot. Dotted lines mark the borders of regions excluded from the sample: the Galactic plane, the circumpolar region, and the Magellanic Clouds.

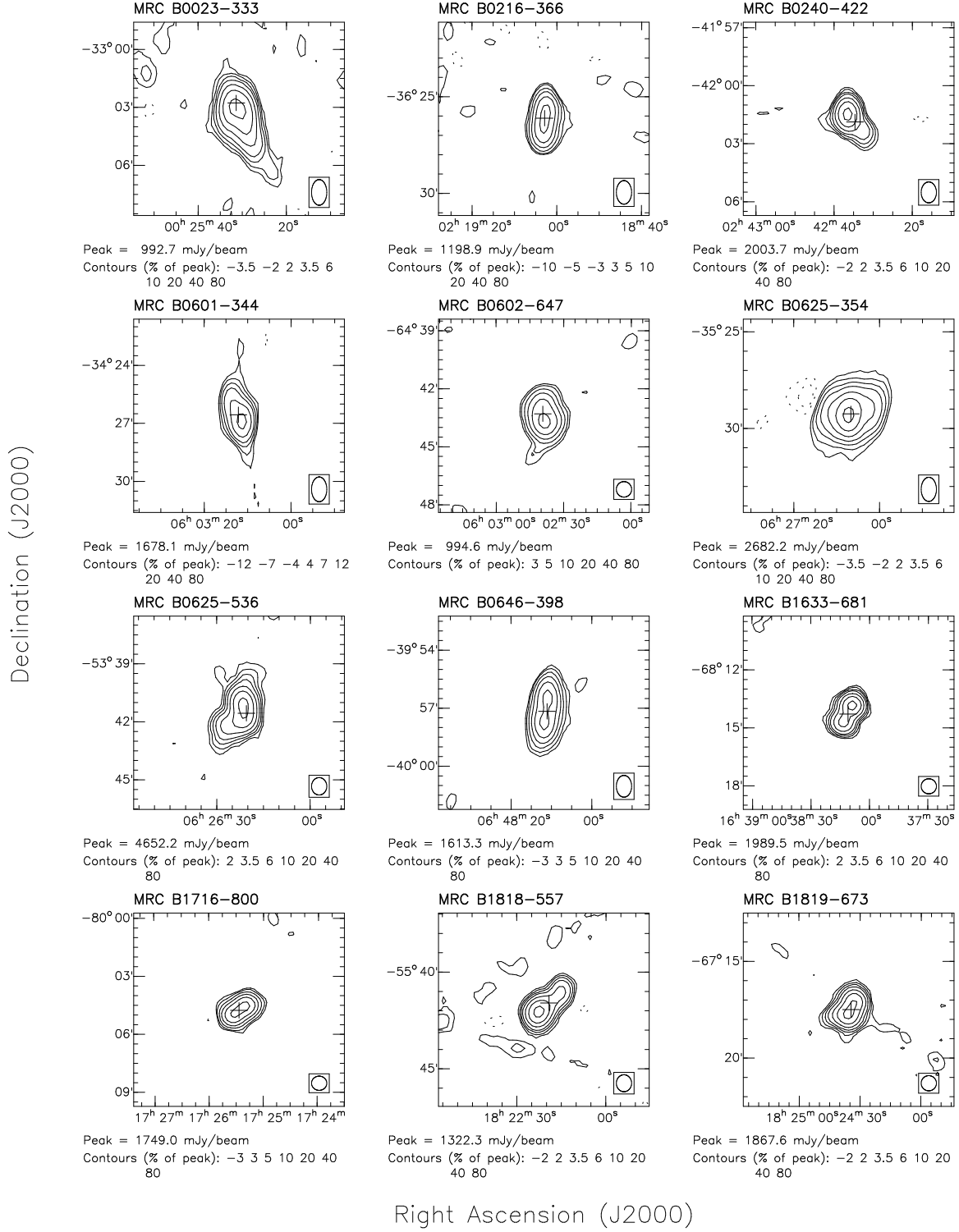


Fig. 2.— 843 MHz contour images of slightly extended MS4 sources, obtained in CUTS observing mode (see § 3.1). The crosses mark the positions of the optical counterparts. The Gaussian restoring beam is shown in the bottom right-hand corner of each plot. The side length of each plot is 10′.

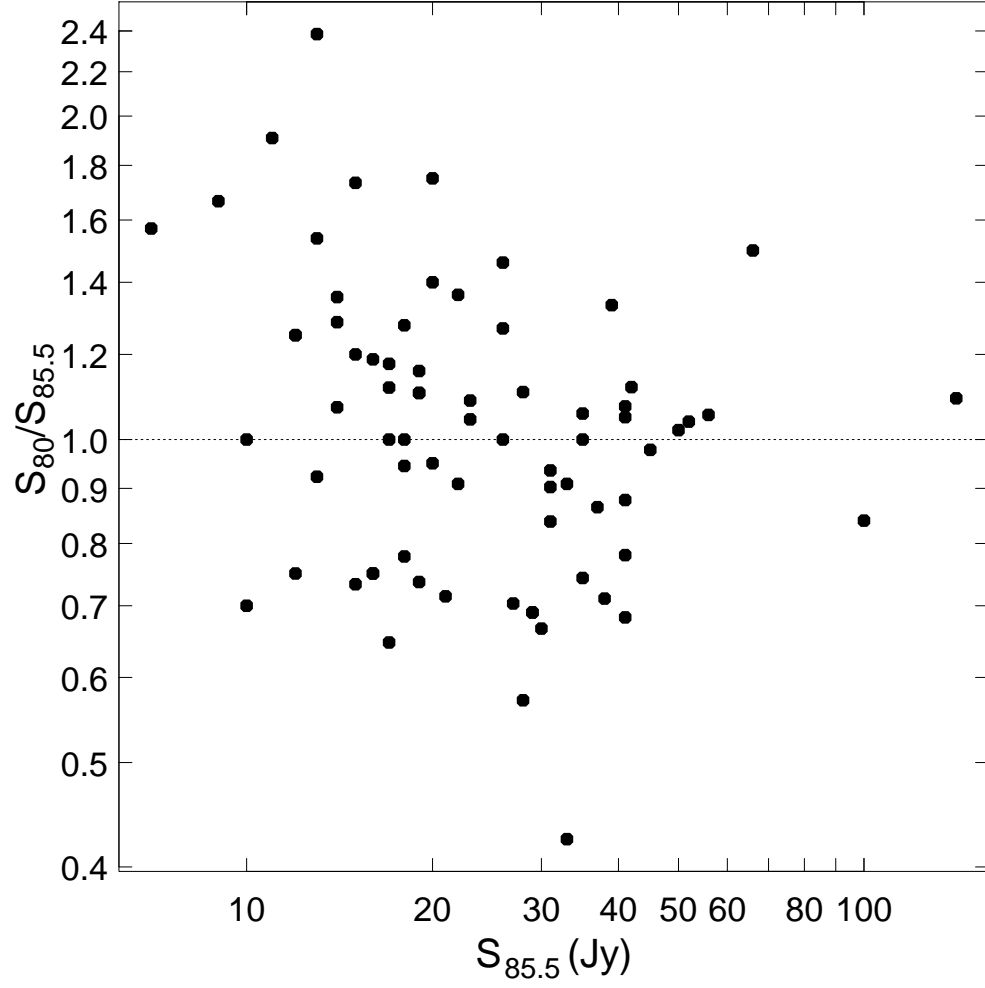


Fig. 3.— Ratio of  $S_{80\text{MHz}}$  to  $S_{85.5\text{MHz}}$  versus  $S_{85.5\text{MHz}}$ . The values at 80 MHz were measured with the Culgoora Circular Array, and those at 85.5 MHz were from the MSH survey.

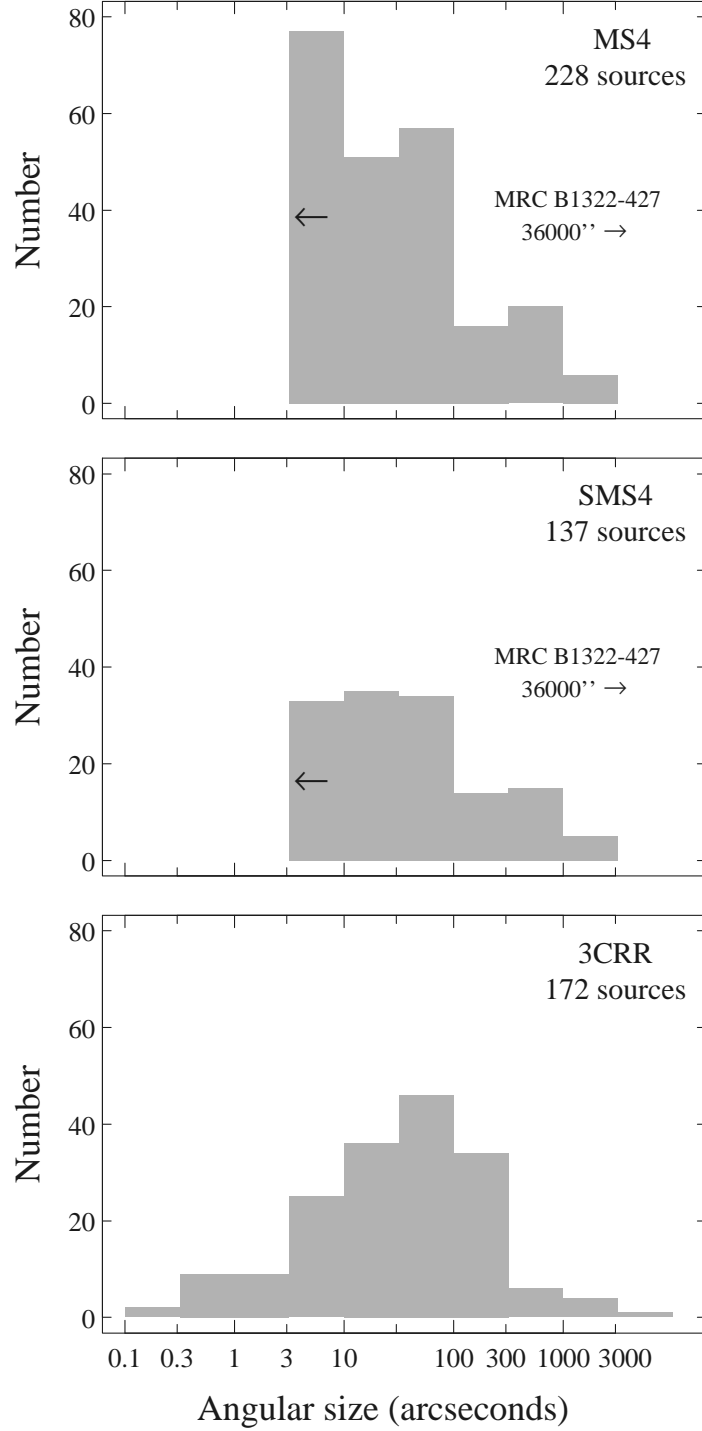


Fig. 4.— Histograms of angular size for the MS4, SMS4, and 3CRR samples. In the MS4 and SMS4 data, MRC B1322–427 is off-scale, and the leftmost bin represents an upper limit to the angular size for many of the sources.

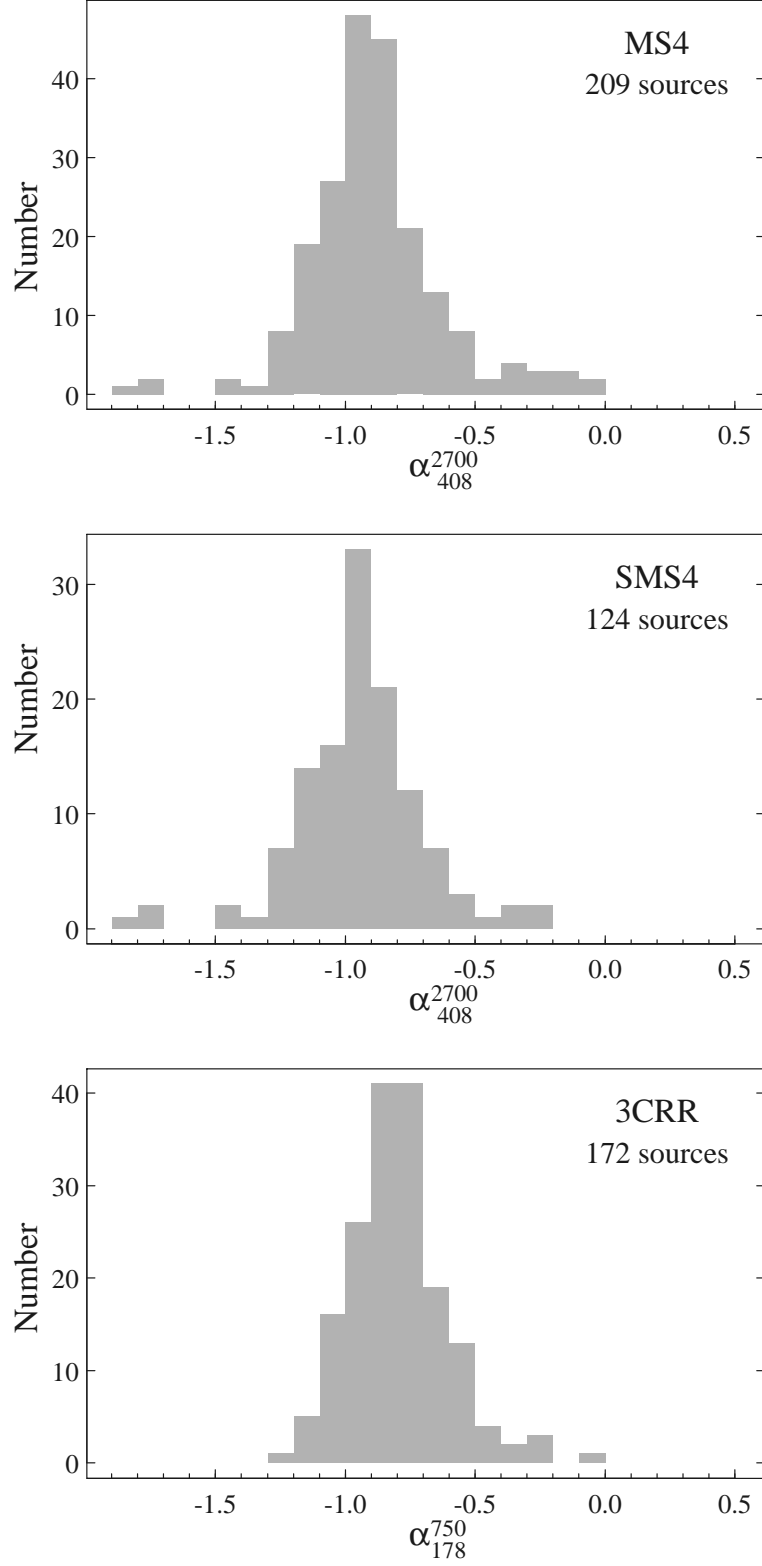


Fig. 5.— Histograms of spectral index for the MS4, SMS4, and 3CRR samples. MS4 and SMS4 sources without reliable flux density data have been omitted.

Table 1. Radio surveys of strong southern extragalactic sources

(1) Survey	(2) Frequency (MHz)	(3) Flux density limit (Jy)	(4) No. of sources	(5) References
MSH	85.5	10	2270	1 2 3
PKS	408 <sup>a</sup>	4 <sup>b</sup>	2133	4 5 6 7 8
PKS 2700	2700	$\sim 0.25^c$	$\sim 6000^d$	9
MRC	408	1.0 <sup>e</sup>	12141	10
PMN	4850	0.04 <sup>f</sup>	50814	11 12 13 14

<sup>a</sup>Price & Milne (1965) made part of their survey at 1410 MHz; the survey of Shimmins & Day (1968) was made at 635 MHz.

<sup>b</sup>The flux-density limit at 408 MHz varied from 3 to 4 Jy; some papers contained additional sources down to  $S_{408} = 1.0$  Jy.

<sup>c</sup>The flux-density limit varies from 0.1 to 0.6 Jy.

<sup>d</sup>The total number of entries in parts 1 to 14 of the catalogue is 6842, but some sources were observed more than once.

<sup>e</sup>Complete to 1 Jy but contains sources down to 0.7 Jy.

<sup>f</sup>The flux-density limit varies from 0.020 to 0.072 Jy with declination.

References. — (1) Mills et al. (1958), (2) Mills et al. (1960), (3) Mills et al. (1961), (4) Bolton et al. (1964), (5) Price & Milne (1965), (6) Day et al. (1966), (7) Shimmins et al. (1966), (8) Shimmins & Day (1968), (9) Bolton et al. (1979) and references therein, (10) Large et al. (1981), (11) Griffith et al. (1994), (12) Wright et al. (1994), (13) Griffith et al. (1995), (14) Wright et al. (1996).

Table 2. Extended sources with MRC  $S_{408} < 4.0$  Jy which have been added to the sample

(1) IAU name	(2) MRC name(s)	(3) LAS (arcmin)	(4) Integrated $S_{408}$ (Jy)	(5) Source of estimate
PKS B0114–47	0113–475, 0114–476	9.5	6.6 <sup>a</sup>	SM75
MRC B0214–480	0214–480	7.1	5.5 <sup>a</sup>	SM75
PKS B0319–45	0319–453, 0317–456	25.6	8.3	Radio spectrum
PKS B0332–39	0332–391A, 0332–391B	7	4.2	SM75
MRC B0424–728	0424–728	3.6	4.3	MC4
MRC B0429–616	0429–616	1.9	4.4 <sup>a</sup>	MC4
PKS B0511–30	0511–305, 0511–304	10.6	7.8	SM75
PKS B0707–35	0707–359A, 0707–359B	8.1	4.6	SM75
MRC B0715–362	0715–362	7.5	5.7	SM75
MRC B1056–360	1056–360	8	4.1	Molonglo Cross
MRC B1259–445	1259–445	2.2	4.4 <sup>a</sup>	Transit catalogue
PKS B1302–325	1302–325A, 1302–325B	5.7	5.3	Transit catalogue
PKS B1318–434	1318–434A, 1318–434B	17	10.0	SM75
PKS B1333–33	1332–336, 1333–337, 1334–339	32	30.8	SM75
PKS B1400–33	...	16	5.8	SM75
MRC B1425–479	1425–479	4.5	4.5	Transit catalogue
MRC B1545–321	1545–321	7.0	9.0	Radio spectrum
MRC B2006–566	2006–566	28	7.3 <sup>a</sup>	SM75
MRC B2013–557	2013–557	20	4.8	SM75
PKS B2148–555	2147–555, 2148–555	13	5.8	Transit catalogue

<sup>a</sup>PKS 408 MHz flux density was preferred.



Table 3. Extended sources found to be just below the 4.0 Jy flux-density limit

(1) Source name	(2) LAS (arcmin)	(3) $S_{408}$ (Jy)	(4) Means of estimate
MRC B0816–705	6	3.5	MC4
MRC B1011–316	1.3	3.9	Transit catalogue
MRC B1148–353	1.8	3.8	Transit catalogue
MRC B1308–441	14.4	$\sim 3.8$	Radio spectrum
MRC B1511–315	2.1	3.8	Radio spectrum
MRC B1821–583	3.3	3.3	SM75

Table 4. List of sources in the MS4 sample.

(1) MRC name(s)	(2) PKS name(s)	(3) MSH name	(4) $S_{408}$ (Jy)	(5) References for radio images
B0003–567	B0003–56	00–51	$5.19 \pm 0.23$	...
B0003–428	B0003–42	00–42	$5.15 \pm 0.16$	...
B0003–833	B0004–83	...	$6.62 \pm 0.31$	1
B0007–446	B0007–44	00–43	$6.81 \pm 0.21$	...
B0008–421	B0008–42	...	$6.61 \pm 0.21$	...
B0012–383	B0012–38	00–35	$4.87 \pm 0.14$	...
B0013–634	B0013–63	00–61	$6.90 \pm 0.17$	...
B0023–333	B0023–33	00–38	$4.09 \pm 0.18$	2
B0036–392	B0035–39	00–313	$5.80 \pm 0.15$	...
B0039–445	B0039–44	00–410	$10.23 \pm 0.31$	3
B0042–357	B0042–35	00–315	$5.79 \pm 0.18$	...
B0043–424	B0043–42	00–411	$21.0 \pm 1.2$	1 3 4 5
B0048–447	B0048–44	00–413	$4.78 \pm 0.15$	...
B0049–433	B0049–43	00–414	$8.07 \pm 0.25$	...
B0103–453	B0103–45	01–41	$7.5 \pm 0.7$	1 4
B0110–692	B0110–69	...	$6.10 \pm 0.19$	1
B0113–475 } B0114–476 }	B0114–47	01–45	$10.4 \pm 0.8$	1 6 7 8 9
B0119–634	B0119–63	01–61	$5.20 \pm 0.23$	...
B0131–449	B0131–44	01–49	$4.03 \pm 0.13$	...
B0131–367A } B0131–367B }	B0131–36	01–311	$17.1 \pm 1.0$	1 2 4 6 10 11 12
B0157–311	B0157–31	01–315	$10.31 \pm 0.45$	12
B0201–440	B0201–44	02–41	$6.17 \pm 0.27$	...
B0202–765	B0202–76	...	$8.46 \pm 0.08$	...
B0208–512	B0208–512	...	$5.48 \pm 0.14$	13
B0214–480	B0214–48	02–43	$9.5 \pm 0.8$	1 6 14 15
B0216–366	B0216–36	02–33	$4.3 \pm 0.3$	6
B0219–706	B0219–706	...	$6.87 \pm 0.29$	...
B0223–712	B0223–71	...	$5.28 \pm 0.23$	...
B0240–422	B0240–42	02–410	$4.22 \pm 0.13$	...
B0241–512	B0241–513	...	$4.45 \pm 0.12$	6
B0242–514	B0241–51	02–53	$7.99 \pm 0.24$	6
B0245–558	B0245–55	02–54	$8.25 \pm 0.36$	...
B0251–675	B0251–67	02–65	$4.85 \pm 0.15$	...
B0252–712	B0252–71	02–72	$14.08 \pm 0.43$	...
B0315–685	B0315–68	...	$5.26 \pm 0.14$	...
B0317–456 } B0319–453 }	B0319–45	03–43	$8.3 \pm 2.0$	1 4 16 17 18
B0320–373	B0320–37	03–31	$259 \pm 26$	1 2 19 20 21 22 23 24 25 26
B0332–391A				

Table 4—Continued

(1) MRC name(s)	(2) PKS name(s)	(3) MSH name	(4) $S_{408}$ (Jy)	(5) References for radio images
B0332–391B } B0335–415 B0336–355	B0332–39 B0335–415 B0336–35	03–32 03–44 03–33	4.2 ± 0.3 4.10 ± 0.50 5.0 ± 0.3	1 2 6 10 27 28 ... 1 2 4 6 23 27 29 30 31 32
B0340–372 B0344–345 B0357–371 B0407–658 B0409–752 B0411–346A B0411–647 B0411–561 B0420–625 B0424–728 B0427–539A } B0427–539B }	B0340–37 B0344–34 B0357–37 B0408–65 B0410–75 B0411–34 B0411–647 B0411–56 B0420–62 B0425–72 B0427–53	... 03–36 03–39 04–62 04–71 04–33 ... 04–52 04–63 04–72 04–54	5.03 ± 0.16 9.3 ± 0.8 4.68 ± 0.15 51.14 ± 1.72 35.97 ± 0.63 4.35 ± 0.20 4.18 ± 0.11 6.79 ± 0.30 11.54 ± 0.18 4.3 ± 0.35 14.6 ± 0.9	... 1 2 4 6 10 27 1 ... 3 5 33 ... ... 5 5 1 8 17 34 1 6 10 12 14 22 35
B0427–366 B0429–616 B0436–650 B0438–436 B0453–301 B0454–463 B0456–301 B0506–612 B0509–573 B0511–484 B0511–304 } B0511–305 }	B0427–36 B0429–61 B0437–65 B0438–43 B0453–30 B0454–46 B0456–30 B0506–61 B0509–573 B0511–48 B0511–30	04–36 04–64 04–65 04–49 ... ... ... 05–61 ... ... 05–35	8.41 ± 1.05 6.5 ± 1.2 4.26 ± 0.14 8.12 ± 0.25 9.16 ± 0.20 4.25 ± 0.13 7.21 ± 0.36 5.03 ± 0.16 5.12 ± 0.22 6.84 ± 0.11 7.8 ± 0.5	... 1 17 34 36 34 37 ... ... 1 4 ... ... 1 6 10 38 1 2 4 6 8 27
B0513–488 B0518–458A } B0518–458B }	B0513–488 B0518–45	... 05–43	4.04 ± 0.11 166 ± 8.3	39 40 ... 1 4 6 14 22 41 42 43 44 45
B0521–365 B0534–497 B0546–445 B0547–408 B0601–344 B0602–319 B0602–647 B0614–349 B0615–365 B0618–371	B0521–36 B0535–49 B0546–44 B0547–40 B0600–34 B0602–31 B0602–64 B0614–34 B0615–365 B0618–37	05–36 05–46 05–48 05–410 06–31 ... ... 06–36 ... 06–37	36.08 ± 1.56 6.69 ± 0.15 4.41 ± 0.14 8.24 ± 0.24 4.40 ± 0.46 6.67 ± 0.29 4.49 ± 0.10 5.29 ± 0.21 4.41 ± 0.20 5.81 ± 0.22	2 46 47 48 49 50 ... ... ... ... 32 ... ... ... ... 1 2 4 41 51

Table 4—Continued

(1) MRC name(s)	(2) PKS name(s)	(3) MSH name	(4) $S_{408}$ (Jy)	(5) References for radio images
B0620–526	B0620–52	06–53	9.3 $\pm$ 0.8	1 12 17
B0625–536	B0625–53	06–55	26 $\pm$ 1.4	3 5 52 53 54
B0625–354	B0625–35	06–38	9.23 $\pm$ 0.70	2 4 27 28
B0625–545	B0625–545	...	7.86 $\pm$ 0.68	1
B0637–752	B0637–75	06–71	7.89 $\pm$ 0.10	37 55 56
B0646–398	B0646–39	06–312	7.0 $\pm$ 0.7	...
B0647–475	B0647–475	...	4.35 $\pm$ 0.11	...
B0658–656	B0658–65	06–64	6.14 $\pm$ 0.24	...
B0700–473	B0700–47	07–41	4.33 $\pm$ 0.11	...
B0704–427	B0704–42	07–43	4.47 $\pm$ 0.12	...
B0707–359A } B0707–359B }	B0707–35	07–34	4.6 $\pm$ 0.3	1 6 8 10 27
B0715–362	B0715–36	07–35	5.7 $\pm$ 0.3	1 4 6 27
B0719–553	B0719–55	07–53	5.63 $\pm$ 0.18	1
B0743–673	B0744–67	...	8.61 $\pm$ 1.04	5 57
B0842–754	B0842–75	08–71	13.35 $\pm$ 0.58	...
B0842–835	B0841–83	...	4.78 $\pm$ 0.21	...
B0846–811	B0846–81	...	4.09 $\pm$ 0.18	...
B0906–682	B0905–68	...	6.11 $\pm$ 0.07	...
B0910–636	B0910–63	...	4.01 $\pm$ 0.10	...
B0943–761	B0943–76	...	4.91 $\pm$ 0.22	...
B1003–415	B1003–415	...	4.07 $\pm$ 0.18	...
B1015–314	B1015–31	...	9.67 $\pm$ 0.35	...
B1017–421	B1017–42	...	5.04 $\pm$ 0.22	4
B1017–325	B1017–325	10–36	4.76 $\pm$ 0.13	...
B1017–426	B1018–42	...	12.72 $\pm$ 0.55	58
B1030–340	B1030–34	10–38	5.59 $\pm$ 0.25	...
B1036–697	B1036–69	...	6.92 $\pm$ 0.27	...
B1044–357	B1044–357	...	4.15 $\pm$ 0.13	...
B1046–409	B1046–409	...	5.02 $\pm$ 0.16	13
B1056–360	B1056–360	10–314	4.09 $\pm$ 0.15	1 2 4 17
B1116–462	B1116–46	...	4.68 $\pm$ 0.21	...
B1123–351	B1123–35	11–33	6.61 $\pm$ 0.28	1 2 4
B1136–320	B1136–32	11–38	6.78 $\pm$ 0.30	1 5
B1143–483	B1143–48	11–46	7.47 $\pm$ 0.23	...
B1143–316	B1143–31	11–310	5.77 $\pm$ 0.25	1 4 6
B1151–348	B1151–34	11–314	10.90 $\pm$ 0.40	32
B1206–337	B1206–337	12–32	4.65 $\pm$ 0.21	...
B1215–457	B1215–45	...	9.59 $\pm$ 0.42	...
B1221–423	B1221–42	...	5.08 $\pm$ 0.13	5 59
B1232–416	B1232–41	...	5.33 $\pm$ 0.24	...
B1234–504	...	...	4.57 $\pm$ 0.08	...
B1243–412	B1243–412	...	4.40 $\pm$ 0.14	...
B1246–410	B1245–41	12–45	10.59 $\pm$ 0.46	60 61 62

Table 4—Continued

(1) MRC name(s)	(2) PKS name(s)	(3) MSH name	(4) $S_{408}$ (Jy)	(5) References for radio images
B1247–401	B1247–40	...	$6.03 \pm 0.18$	...
B1259–769	B1259–76	...	$4.15 \pm 0.13$	...
B1259–445	B1259–44	...	$4.2 \pm 0.6$	1
B1302–325A } B1302–325B }	B1302–325	...	$5.27 \pm 1.42$	1 17
B1302–491	B1302–49	13–41	$12.6 \pm 1.26$	1 23 63 64 65 66 67 68 69 70 71 72
B1303–827	B1302–82	...	$4.84 \pm 0.22$	...
B1315–460	...	...	$6.24 \pm 0.27$	...
B1318–434A } B1318–434B }	B1318–434	...	$10.0 \pm 0.6$	1 6 10 12 73 74 75 76
B1320–446	B1320–446	...	$6.91 \pm 0.55$	...
B1322–427	B1322–42	13–42	$2740 \pm 548$	1 4 13 14 19 20 21 22 23 39 41 42 77 78 79 80 81 82 83 84 85 86 87 88 89 90 91 92 93 94 95 96 97 98 99 100
B1330–328	B1330–328	...	$4.27 \pm 0.14$	36
B1332–336 } B1333–337 } B1334–339 }	{ B1332–33 } { B1333–33 } { B1334–33 }	13–33	$30.8 \pm 1.8$	1 2 4 6 12 22 40 101 40 101
B1346–391	B1346–39	13–44	$5.84 \pm 0.26$	...
B1355–416	B1355–41	13–45	$12.9 \pm 0.6$	1 5
B1358–493	...	...	$6.46 \pm 0.28$	...
B1359–358	B1359–35	...	$4.47 \pm 0.14$	...
...	B1400–33	14–32	$5.8 \pm 0.3$	2 6 10 27 102 103 104
B1407–425	B1407–425	...	$4.67 \pm 0.21$	...
B1413–364	B1413–36	...	$5.71 \pm 0.22$	1 2 4
B1416–493	B1416–49	...	$7.34 \pm 0.32$	...
B1421–382	B1421–38	14–34	$6.92 \pm 0.21$	1
B1421–490	...	...	$13.10 \pm 0.67$	...
B1424–418	B1424–41	...	$6.39 \pm 0.28$	13
B1425–479	...	14–46	$4.45 \pm 0.37$	1 17
B1445–468	B1445–46	14–49	$6.97 \pm 0.31$	...
B1451–364	B1451–36	14–38	$8.99 \pm 0.72$	1 4 5
B1458–391	...	...	$6.07 \pm 0.19$	...
B1526–423	...	15–43	$17.86 \pm 1.38$	...
B1540–730	B1540–73	...	$5.33 \pm 0.14$	...
B1540–337	B1540–337	...	$4.33 \pm 0.19$	...
B1545–321	B1545–321	...	$9.0 \pm 2.2$	1 4 8 17 105

Table 4—Continued

(1) MRC name(s)	(2) PKS name(s)	(3) MSH name	(4) $S_{408}$ (Jy)	(5) References for radio images
B1547–795	B1547–79	...	$10.45 \pm 0.57$	5
B1549–790	B1549–79	...	$7.95 \pm 0.35$	...
B1607–841	B1606–84	...	$4.91 \pm 0.22$	...
B1610–771	B1610–77	...	$5.35 \pm 0.17$	...
B1622–310	B1622–31	...	$5.20 \pm 0.23$	32
B1633–681	B1632–68	...	$6.66 \pm 0.29$	...
B1637–771	B1637–77	...	$13.5 \pm 1.4$	1 12 17
B1655–776	B1655–77	...	$5.04 \pm 0.22$	13
B1706–606	...	...	$5.54 \pm 0.17$	...
B1716–800	B1716–80	...	$5.91 \pm 0.26$	...
B1721–836	B1720–83	...	$4.63 \pm 0.21$	...
B1733–565A } B1733–565B }	B1733–56	...	$20.3 \pm 1.2$	1 6 12 14 41 106 107
B1737–575	B1737–575	...	$5.12 \pm 0.64$	...
B1737–609	B1737–60	...	$8.32 \pm 0.21$	1
B1740–517	B1740–517	...	$5.38 \pm 0.12$	...
B1754–597	B1754–59	17–51	$12.58 \pm 0.55$	...
B1756–663	B1756–663	...	$5.46 \pm 0.22$	...
B1814–519	B1814–51	18–52	$14.26 \pm 0.28$	...
B1814–637	B1814–63	...	$37.00 \pm 1.34$	...
B1817–391	...	18–33	$9.74 \pm 0.24$	108
B1817–640	B1817–64	...	$11.50 \pm 0.35$	...
B1818–557	B1818–557	18–53	$4.14 \pm 0.19$	...
B1819–673	B1819–67	...	$6.06 \pm 0.19$	5
B1827–360	B1827–36	...	$25.83 \pm 0.79$	...
B1829–344	B1829–344	...	$4.19 \pm 0.19$	...
B1831–668	B1831–668	...	$4.28 \pm 0.14$	...
B1839–487	B1839–48	18–43	$9.08 \pm 0.23$	12
B1840–404	B1840–40	18–44	$8.44 \pm 0.24$	1 5
B1853–303	B1853–303	...	$5.09 \pm 0.23$	...
B1854–663	B1855–66	...	$4.41 \pm 0.14$	...
B1917–546	B1917–54	19–52	$4.59 \pm 0.21$	...
B1922–627	B1922–62	19–61	$4.88 \pm 0.20$	1
B1923–328	B1923–328	...	$4.25 \pm 0.18$	...
B1929–397	B1929–397	...	$6.41 \pm 0.27$	1 2 4 27
B1932–464	B1932–46	19–46	$39.61 \pm 0.83$	5 109
B1933–587	B1933–58	19–56	$9.13 \pm 0.40$	...
B1934–638	B1934–63	...	$6.24 \pm 0.20$	...
B1940–406	B1940–40	19–410	$5.7 \pm 0.3$	1 4 6 110
B1953–425	B1953–42	19–413	$10.13 \pm 0.95$	...
B1954–552	B1954–55	19–57	$14.8 \pm 1.0$	1 3 5 14
B1955–357	B1955–35	19–35	$4.86 \pm 0.15$	...
B2006–566	B2006–56	20–52	$12.2 \pm 0.9$	1 6 10 111 112

Table 4—Continued

(1) MRC name(s)	(2) PKS name(s)	(3) MSH name	(4) $S_{408}$ (Jy)	(5) References for radio images
B2009–524	B2009–52	20–53	$4.52 \pm 0.12$	...
B2013–557	B2014–55	20–54	$4.8 \pm 0.3$	1 6 10 27
B2020–575	B2020–57	20–55	$9.89 \pm 0.39$	1 5
B2028–732	B2028–73	20–71	$4.57 \pm 0.15$	1
B2031–359	B2031–359	...	$4.40 \pm 0.11$	2
B2032–350	B2032–35	20–37	$17.60 \pm 0.76$	...
B2041–604	B2041–60	20–61	$11.16 \pm 0.34$	1 110
B2049–368	B2049–36	...	$5.75 \pm 0.18$	...
B2052–474	B2052–47	...	$4.15 \pm 0.10$	13
B2059–641	B2059–64	20–62	$4.24 \pm 0.17$	...
B2115–305	B2115–30	21–34	$6.89 \pm 0.30$	32
B2122–555	B2122–555	21–52	$4.05 \pm 0.18$	...
B2128–315	B2128–315	21–36	$4.18 \pm 0.13$	32
B2140–434	B2140–43	21–47	$9.18 \pm 0.28$	5
B2140–817	B2141–81	...	$8.72 \pm 1.01$	5
B2147–555 } B2148–555 }	B2148–555	...	$5.8 \pm 1.0$	1 17 113
B2150–520	B2150–52	21–58	$10.08 \pm 0.20$	5
B2152–699	B2153–69	...	$61.6 \pm 3.7$	1 6 14 41 114 115 116 117 118
B2153–699	...	...	$11.9 \pm 2.0$	1 6 14 41 114 115 116 118
B2158–380	B2158–380	21–38	$4.12 \pm 0.14$	1 2 119
B2201–555	B2201–55	...	$5.56 \pm 0.25$	...
B2213–456	B2213–45	...	$4.33 \pm 0.10$	...
B2223–528	B2223–52	22–52	$8.83 \pm 0.38$	...
B2226–411	B2226–41	...	$6.83 \pm 0.79$	1
B2226–386	B2226–38	...	$8.21 \pm 0.21$	...
B2250–412	B2250–41	22–46	$13.93 \pm 0.60$	5 12 120
B2252–530	B2252–53	22–54	$6.37 \pm 0.28$	1
B2253–522	B2253–52	...	$7.20 \pm 0.18$	...
B2259–375	B2259–37	22–35	$7.47 \pm 0.16$	...
B2305–418	B2305–41	...	$4.02 \pm 0.18$	...
B2319–550	B2319–55	...	$5.73 \pm 0.25$	...
B2323–407	B2323–40	23–43	$9.28 \pm 0.40$	...
B2331–416	B2331–41	23–44	$15.92 \pm 0.69$	...
B2332–668	B2332–66	23–63	$5.93 \pm 0.26$	...
B2338–585	B2338–58	23–52	$8.17 \pm 0.21$	...
B2339–353	B2339–353	...	$5.67 \pm 0.22$	121
B2354–350	B2354–35	23–37	$8.70 \pm 0.35$	2 13 122 123 124
B2356–611 } B2356–612A } B2356–612B }	B2356–61	23–64	$61.2 \pm 3.7$	1 6 8 14 41 114 117 125

Table 4—Continued

(1)	(2)	(3)	(4)	(5)
MRC	PKS	MSH	$S_{408}$	References for
name(s)	name(s)	name	(Jy)	radio images

References. — (1) JM92; (2) Ekers et al. (1989); (3) Morganti et al. (1999b); (4) Slee (1977); (5) Duncan & Sproats (1992); (6) SM75; (7) Danziger & Goss (1983); (8) Subrahmanyam et al. (1996); (9) Saripalli et al. (2002); (10) Wall & Schilizzi (1979); (11) Ekers et al. (1978); (12) Morganti et al. (1993); (13) Choi et al. (2004); (14) Christiansen et al. (1977); (15) White et al. (1984); (16) Jones (1989a); (17) Jones (1992); (18) Saripalli et al. (1994); (19) Sheridan (1958); (20) Shain (1958); (21) Heeschen (1961); (22) Gardner & Whiteoak (1971); (23) Cameron (1971); (24) Ekers et al. (1983); (25) Geldzahler & Fomalont (1984); (26) Fomalont et al. (1989); (27) Smith (1983); (28) Marvel et al. (1999); (29) Carter & Malin (1983); (30) Harnett (1987); (31) Killeen & Bicknell (1988); (32) Reid et al. (1999); (33) Reynolds et al. (1993); (34) Clarke et al. (1976); (35) McAdam et al. (1988); (36) Unewisse (1993); (37) Tingay et al. (1998); (38) Robertson & Smith (1981); (39) Wall & Cole (1973); (40) Swarup (1984); (41) Schwarz et al. (1974); (42) Slee & Sheridan (1975); (43) Meisenheimer et al. (1989); (44) Perley et al. (1997); (45) Simkin et al. (1999); (46) Wardle et al. (1984); (47) Keel (1986); (48) Drinkwater et al. (1997); (49) Hardcastle et al. (1999); (50) Birkinshaw et al. (2002); (51) Parma et al. (1991); (52) Gregorini et al. (1994); (53) Otani et al. (1998); (54) Gliozzi et al. (1999); (55) Chartas et al. (2000); (56) Schwartz et al. (2000); (57) Rayner et al. (2000); (58) Ulvestad et al. (1981); (59) Safouris et al. (2003); (60) Sadler (1987); (61) O’Dea et al. (1994); (62) Taylor et al. (2002); (63) Bosma et al. (1983); (64) Harnett & Reynolds (1985); (65) Whiteoak & Bunton (1985); (66) Harnett et al. (1989); (67) Harnett et al. (1990); (68) Whiteoak & Wilson (1990); (69) Dahlem et al. (1993); (70) Elmouttie et al. (1997); (71) Forbes & Norris (1998); (72) Ott et al. (2001); (73) Smith & Bicknell (1983); (74) Smith & Bicknell (1986); (75) Lloyd et al. (1996); (76) Morganti et al. (2001); (77) McGee et al. (1955); (78) Bolton & Clark (1960); (79) Cooper et al. (1965); (80) Lockhart & Sheridan (1970); (81) Kaufmann et al. (1974); (82) Schreier et al. (1981); (83) Haslam et al. (1981); (84) Slee et al. (1983); (85) Burns et al. (1983); (86) Haynes et al. (1983); (87) Van Gorkom et al. (1990); (88) Clarke et al. (1992); (89) Tateyama & Strauss (1992); (90) Junkes et al. (1993a); (91) Junkes et al. (1993b); (92) Schiminovich et al. (1994); (93) Condon et al. (1996); (94) Combi & Romero (1997); (95) Morganti et al. (1999a); (96) Alvarez et al. (2000); (97) Kraft et al. (2002); (98) Sarma et al. (2002); (99) Hardcastle et al. (2003); (100) Kraft et al. (2003); (101) Killeen et al. (1986); (102) McAdam & Schilizzi (1977); (103) Goss et al. (1987); (104) Subrahmanyam et al. (2003); (105) Saripalli et al. (2003); (106) Hunstead et al. (1982); (107) Sault & Wieringa (1994); (108) de Pater et al. (1985); (109) Villar-Martín et al. (1998); (110) De Breuck et al. (2000); (111) Goss et al. (1982); (112) Röttgering et al. (1997); (113) Lloyd & Jones (2002); (114) Schwarz et al. (1973); (115) Tadhunter et al. (1988); (116) Norris et al. (1990); (117) Ekers & Whiteoak (1992); (118) Fosbury et al. (1998); (119) Fosbury et al. (1982); (120) Clark et al. (1997); (121) De Breuck et al. (2004); (122) Schwartz et al. (1991); (123) Taylor et al. (1994); (124) Heinz et al. (2002); (125) Sadler (1997).



Table 5. Radio positions, flux densities, angular sizes, and position angles for the MS4 sample.

(1)	(2)	(3)	(4)	(5)	(6)	(7)	(8)	(9)	(10)	(11)	(12)	(13)		
Source	RA (J2000)	Dec	Flux density (Jy)			Flux density (Jy)			Flux density (Jy)			$\alpha_{408}^{2700}$	LAS <sup>a</sup>	P.A.
name	h m s	° ' "	$S_{178}$	$S_{80}$	$S_{408}$	$S_{843}$	$S_{1400}$	$S_{2700}$	$S_{5000}$		"	°		
MRC B0003–567	00 05 57.64	−56 28 30.6	8.6 2	12 [2]	5.19 [3]	2.88 [4]	2.0 [5]	1.08 [6]	0.69 [7]	−0.83	19 m	−72		
MRC B0003–428	00 06 01.96	−42 34 41.9	9.5 2	17 [8]	5.15 [3]	2.97 [4]	1.7 [5]	1.02 [9]	0.53 [7]	−0.86	≤10 m	...		
MRC B0003–833	00 06 14.6	−83 05 60	13.2: 1	...	6.62 [3]	3.40 [10]	2.5 <sup>i</sup> [11]	1.19 [12]	0.84 [7]	−0.91	60 d	−24		
MRC B0007–446	00 10 30.50	−44 22 56.4	15 2	26 [13]	6.81 [3]	3.26 [4]	1.7 [5]	0.82 [9]	0.36 [7]	−1.12	33 m	65		
MRC B0008–421	00 10 52.55	−41 53 10.3	2.69:3	...	6.61 [3]	6.52 [1]	4.62 [14]	2.49 [14]	1.32 [14]	−0.52	≤10 m	...		
MRC B0012–383	00 15 24.33	−38 04 33.6	10.7 2	21 [13]	4.87 [3]	2.18 [4]	1.26 [15]	0.65 [9]	0.35 [7]	−1.07	20 m	78		
MRC B0013–634	00 16 02.59	−63 10 06.6	15 2	27 [2]	6.90 [3]	3.07 [4]	1.9 [11]	0.82 [6]	0.45 [7]	−1.13	31 m	76		
MRC B0023–333	00 25 30.89	−33 03 21.1	9.3 2	19 [13]	4.09 [3]	2.18 [4]	1.37 [15]	0.73 [16]	0.4 [17]	−0.91	68 ℓ	17		
MRC B0036–392	00 38 26.89	−38 59 46.7	12.7 2	20 [13]	5.80 [3]	2.75 [1]	1.63 [15]	0.85 [9]	0.49 [7]	−1.02	≤10 m	...		
MRC B0039–445	00 42 08.97	−44 13 59.4	19 3	26 [13]	10.23 [3]	5.97 [4]	3.55 [18]	2.08 [9]	1.18 [7]	−0.84	11 m	−70		
MRC B0042–357	00 44 41.43	−35 30 31.8	9.7 2	20 [13]	5.79 [3]	3.73 [1]	2.57 [18]	1.64 [9]	0.98 [19]	−0.67	≤10 m	...		
MRC B0043–424	00 46 16.74	−42 07 39.3	35 1	52 [8]	21.0 [5]	11.26 [4]	8.14 [14]	5.05 [14]	3.35 [14]	−0.76	127 d	−44		
MRC B0048–447	00 50 51.99	−44 28 38.9	10.1 2	19 [13]	4.78 [3]	2.40 [1]	1.6 <sup>i</sup> [5]	0.68 [9]	0.33 [7]	−1.03	≤10 m	...		
MRC B0049–433	00 52 14.79	−43 06 28.4	15 2	24 [13]	8.07 [3]	4.31 [4]	2.74 [18]	1.56 [9]	0.92 [7]	−0.87	18 m	−88		
MRC B0103–453	01 05 20.88	−45 05 28.2	19 1	41 [8]	7.5 [5]	4.32 [4]	2.1 [20]	1.10 [6]	0.65 [7]	−1.02	140 d	54		
MRC B0110–692	01 11 42.88	−68 59 59.3	12.2: 2	...	6.10 [3]	2.98 [4]	2.0 [11]	0.95 [21]	0.51 [7]	−0.98	56 d	−10		
PKS B0114–47	01 16 21.9	−47 22 24	20 2	34 [8]	10.4 [5]	5.48 [22]	2.97 [22]	...	0.75 [7]	−1.06 <sup>b</sup>	570 e	−24		
MRC B0119–634	01 21 40.36	−63 09 02.0	11.4 2	22 [2]	5.20 [3]	2.56 [4]	1.6 [11]	0.73 [6]	0.39 [7]	−1.04	43 m	7		
MRC B0131–449	01 33 33.45	−44 44 21.6	8.3 2	17 [13]	4.03 [3]	2.75 [4]	1.73 [20]	1.09 [9]	0.76 [7]	−0.69	36 d	−80		
PKS B0131–36	01 33 56.5	−36 29 08	30 1	56 [8]	17.1 [23]	10.3 [10]	8.4 [20]	5.6 [9]	4.08 [24]	−0.59	612 e	−83		
MRC B0157–311	02 00 12.12	−30 53 24.1	19 2	38 [13]	10.31 [3]	5.62 [4]	3.70 [18]	2.31 [14]	1.44 [14]	−0.80	14 m	80		
MRC B0201–440	02 03 40.76	−43 49 51.4	9.0 2	15 [13]	6.17 [3]	4.08 [1]	2.62 [18]	1.70 [9]	0.98 [7]	−0.68	≤10 m	...		
MRC B0202–765	02 02 13.53	−76 20 06.8	19: 1	...	8.46 [3]	4.04 [4]	2.51 [14]	1.37 [12]	0.83 [14]	−0.96	20 m	90		
MRC B0208–512	02 10 46.13	−51 01 01.9	6.4: 1	...	5.48 [3]	4.10 <sup>j</sup> [1]	3.89 [25]	3.56 [6]	3.3 [7]	−0.23	≤10 m	...		
MRC B0214–480	02 16 46.55	−47 49 23.0	26 2	65 [8]	9.5 [5]	3.9 <sup>i</sup> [4]	2.5 [20]	1.33 [6]	0.88 <sup>i</sup> [7]	−1.04	426 e	−5		
MRC B0216–366	02 19 02.68	−36 26 11.3	10.6 2	20 [13]	4.3 [23]	1.97 [4]	1.4 <sup>i</sup> [5]	0.69 [9]	0.41 [17]	−0.97	62 d	−9		
MRC B0219–706	02 20 07.96	−70 22 29.2	16: 1	...	6.87 [3]	3.11 [4]	...	1.00 [21]	0.55 [7]	−1.02	≤10 m	...		
MRC B0223–712	02 23 57.29	−70 59 47.2	14: 1	...	5.28 [3]	2.29 [4]	1.5 <sup>i</sup> [11]	0.57 [21]	0.28 [7]	−1.18	23 m	−58		

Table 5—Continued

(1) Source name	(2) RA (J2000) h m s			(3) Dec ° ' "			(4)			(5)			(6)			(7) Flux density (Jy)			(8)			(9)			(10)			(11) $\alpha_{408}^{2700}$			(12) LAS <sup>a</sup> "			(13) P.A. °		
							$S_{178}$			$S_{80}$			$S_{408}$			$S_{843}$			$S_{1400}$			$S_{2700}$			$S_{5000}$											
MRC B0240–422	02	42	36.11	–42	01	34.6	8.2	3	15	[13]	4.22	[3]	2.29	[4]	1.4	[5]	0.81	[9]	0.47	[7]	–0.87	70 d	40													
MRC B0241–512	02	43	13.75	–51	05	17.1	8.9:	1	...	...	4.45	[3]	2.50	[4]	...	...	...	...	0.56	[6]	–0.83 <sup>b</sup>	≤10 m	...													
MRC B0242–514	02	43	44.56	–51	12	36.7	19	2	37	[2]	7.99	[3]	3.62	[4]	...	...	0.86	[6]	0.50	[7]	–1.18	53 m	0													
MRC B0245–558	02	46	56.35	–55	41	24.6	21	2	48	[2]	8.25	[3]	3.88	[4]	2.4	[5]	1.20	[6]	0.55	[6]	–1.02	38 d	–84													
MRC B0251–675	02	51	56.30	–67	18	02.6	13.5	2	34	[2]	4.85	[3]	1.90	[4]	1.2	[11]	0.56	[21]	0.32	[7]	–1.14	38 m	87													
MRC B0252–712	02	52	46.28	–71	04	35.8	13.4	3	7	[2]	14.08	[3]	9.21	[1]	5.9	[11]	3.10	[21]	1.68	[7]	–0.80	≤10 m	...													
MRC B0315–685	03	16	10.55	–68	21	05.9	11.3:	2	...	...	5.26	[3]	2.53	[4]	1.5	[11]	0.70	[21]	0.35	[7]	–1.07	≤10 m	...													
PKS B0319–45	03	21	08.1	–45	12	51	13.5	1	19	[8]	8.3 <sup>h</sup>	...	5.35	[26]	3.83	[26]	...	...	1.20	[7]	–0.85 <sup>c</sup>	1536 e	49													
MRC B0320–373	03	22	43.0	–37	11	40	528	1	950	[8]	259	[27]	169 <sup>h</sup>	...	110	[28]	98 <sup>i</sup>	[9]	...	...	–0.51	2880 $\ell$	–81													
PKS B0332–39	03	34	07.2	–39	00	03	7.3	2	10	[8]	4.2	[23]	2.41	[10]	1.79	[14]	0.90	[9]	0.74 <sup>i</sup>	[24]	–0.82	420 $\ell$	...													
MRC B0335–415	03	37	04.55	–41	23	14.9	9.8	3	19	[13]	4.10	[3]	1.97	[4]	...	...	0.57	[9]	0.29	[7]	–1.04	35 m	–14													
MRC B0336–355	03	38	46.0	–35	22	39	11.0	2	25	[13]	5.0	[23]	2.92	[10]	1.88	[29]	1.40 <sup>i</sup>	[14]	0.71	[14]	–0.68	90 d	41													
MRC B0340–372	03	42	05.38	–37	03	21.8	8.5	3	12	[13]	5.03	[3]	3.09	[1]	2.06	[15]	1.14	[9]	0.82	[7]	–0.79	≤10 m	...													
MRC B0344–345	03	46	31.1	–34	22	40	18	2	33	[8]	9.3	[5]	5.12	[10]	3.80	[29]	2.08	[16]	1.39	[24]	–0.79	264 e	–75													
MRC B0357–371	03	59	46.90	–37	00	30.4	9.4	3	15	[13]	4.68	[3]	2.43	[4]	1.55	[15]	0.82	[9]	0.51	[7]	–0.92	45 m	–38													
MRC B0407–658	04	08	20.35	–65	45	09.5	59	3	36	[2]	51.14	[3]	26.33	[1]	15.75	[14]	7.39	[14]	3.29	[14]	–1.03	≤10 m	...													
MRC B0409–752	04	08	48.34	–75	07	20.3	62	3	87	[2]	35.97	[3]	19.80	[1]	13.78	[14]	7.61	[14]	4.31	[14]	–0.82	≤10 m	...													
MRC B0411–346A	04	13	00.90	–34	30	10.9	8.5	2	12	[13]	4.35	[3]	2.39	[4]	1.45	[15]	0.77	[16]	0.34	[16]	–0.92	≤10 m	...													
MRC B0411–647	04	11	59.30	–64	36	25.1	9.3:	1	...	...	4.18	[3]	2.26	[4]	...	...	0.71	[6]	0.39	[7]	–0.94	35 m	–28													
MRC B0411–561	04	12	48.14	–56	00	48.6	11.3	2	16	[2]	6.79	[3]	3.69	[4]	2.5	[5]	1.39	[14]	0.76	[14]	–0.85	27 m	–7													
MRC B0420–625	04	20	56.09	–62	23	39.6	24	2	38	[2]	11.54	[3]	5.62	[1]	3.0	[11]	1.68	[6]	0.93	[7]	–1.02	≤10 m	...													
MRC B0424–728	04	23	56.5	–72	45	58	7.8	2	11	[2]	4.3	[30]	3.27	[22]	1.7	[11]	...	...	0.45	[7]	–0.91 <sup>b</sup>	216 d	–17													
PKS B0427–53	04	28	59.4	–53	49	39	28	2	50	[2]	14.6	[5]	8.41	[10]	5.83	[14]	3.84	[14]	2.66	[24]	–0.71	276 e	82													
MRC B0427–366	04	29	40.17	–36	30	55.2	18	2	35	[13]	8.41	[3]	3.78	[4]	2.11	[15]	1.02	[9]	0.45	[17]	–1.12	14 m	–27													
MRC B0429–616	04	30	14.9	–61	32	49	15	2	35	[2]	6.5	[11]	2.79	[10]	1.7	[11]	1.07	[6]	0.59	[7]	–0.95	114 d	14													
MRC B0436–650	04	37	08.84	–64	58	55.9	8.7	2	16	[2]	4.26	[3]	2.00	[4]	1.4	[11]	0.70	[21]	0.36	[7]	–0.96	42 m	23													
MRC B0438–436	04	40	17.18	–43	33	09.1	9.7	2	9	[13]	8.12	[3]	6.43	[1]	6.83	[14]	6.17	[14]	6.05	[14]	–0.15	≤10 m	...													

Table 5—Continued

(1) Source name	(2) RA (J2000)			(3) Dec			(4)			(5)			(6)			(7) Flux density (Jy)			(8)			(9)			(10)			(11) $\alpha_{408}^{2700}$	(12) LAS <sup>a</sup>	(13) P.A.
	h	m	s	°	'	"	$S_{178}$			$S_{80}$			$S_{408}$			$S_{843}$			$S_{1400}$			$S_{2700}$			$S_{5000}$				"	°
MRC B0453–301	04	55	14.33	–30	06	48.5	18	2		31	[13]		9.16	[3]		5.07	[4]		3.31	[18]		1.93	[16]		1.19	[19]		–0.82	50 m	–1
MRC B0454–463	04	55	50.76	–46	15	59.0	9.3	2		13	[13]		4.25	[3]		3.00	[4]		2.22	[18]		2.36 <sup>i</sup>	[6]		1.57 <sup>i</sup>	[7]		–0.31	≤10 m	...
MRC B0456–301	04	58	26.43	–30	07	22.4	13.3	2		27	[13]		7.2	[31]		3.89	[4]		2.6	[20]		1.67	[16]		0.90 <sup>i</sup>	[19]		–0.77	348 $\ell$	2
MRC B0506–612	05	06	43.80	–61	09	41.0	8.8	2		14	[2]		5.03	[3]		2.96	[4]		2.2	[11]		1.5	[5]		1.17	[7]		–0.65	≤10 m	...
MRC B0509–573	05	10	18.55	–57	19	41.5	10.3:	1		...	...		5.12	[3]		2.63	[1]		1.64	[25]		0.97	[6]		0.60	[7]		–0.88	≤10 m	...
MRC B0511–484	05	12	50.79	–48	24	04.3	12.2:	1		...	...		6.84	[3]		4.44	[4]		3.3	[20]		1.80	[6]		1.81 <sup>i</sup>	[24]		–0.71	132 d	70
PKS B0511–30	05	13	34.6	–30	28	24	16	2		29	[8]		7.8	[23]		4.90	[22]		3.65	[14]		3.21 <sup>i</sup>	[16]		1.48	[14]		–0.47	636 e	27
MRC B0513–488	05	14	33.20	–48	45	30.5	9.3:	1		...	...		4.04	[3]		1.87	[4]		...	...		0.64	[6]		0.32	[7]		–0.98	43 m	–38
PKS B0518–45	05	19	46.0	–45	46	33	349	2		570	[8]		166	[5]		85.7 <sup>i</sup>	[10]		68.8	[14]		29			15	[6]		–0.92	432 e	–77
MRC B0521–365	05	22	57.97	–36	27	28.2	61	1		99	[13]		36.08	[3]		22.80	[4]		17.50	[14]		11.71	[14]		8.49	[14]		–0.60	19 m	–72
MRC B0534–497	05	36	13.69	–49	44	21.6	11.9	2		16	[8]		6.69	[3]		3.29	[4]		2.1	[5]		1.0	[5]		0.58	[7]		–1.02	30 m	60
MRC B0546–445	05	47	37.98	–44	31	12.0	11.4	2		31	[13]		4.41	[3]		2.56	[4]		1.5	[5]		0.71	[9]		0.41	[7]		–0.97	14 m	3
MRC B0547–408	05	49	23.57	–40	51	14.6	16	2		28	[13]		8.24	[3]		4.72	[4]		2.55	[18]		1.29	[9]		0.87	[7]		–0.98	37 m	–63
MRC B0601–344	06	03	11.85	–34	26	40.7	10.4	2		20	[13]		4.40	[3]		2.52	[4]		1.7	[5]		0.83	[16]		0.41 <sup>i</sup>	[16]		–0.88	64 d	30
MRC B0602–319	06	04	14.53	–31	55	57.6	10.8	2		19	[13]		6.67	[3]		3.93	[4]		2.93	[18]		1.89	[16]		1.18 <sup>i</sup>	[19]		–0.67	12 m	...
MRC B0602–647	06	02	38.65	–64	43	29.4	7.1:	2		...	...		4.49	[3]		2.65	[4]		1.4	[11]		0.70	[32]		0.31	[7]		–0.98	70 m	8
MRC B0614–349	06	16	35.94	–34	56	17.6	7.6	2		11	[13]		5.29	[3]		3.73	[1]		2.91	[14]		1.91	[14]		1.35	[14]		–0.54	≤10 m	...
MRC B0615–365	06	17	32.19	–36	34	15.2	6.8	2		11	[13]		4.41	[3]		2.92	[4]		2.07	[15]		1.17	[9]		0.65	[9]		–0.70	≤10 m	...
MRC B0618–371	06	20	00.55	–37	11	40.8	10.7	2		18	[13]		5.81	[33]		3.80	[4]		2.97	[14]		1.94	[14]		1.31	[14]		–0.59	78 d	81
MRC B0620–526	06	21	41.53	–52	41	15.5	17	2		30	[2]		9.3	[5]		5.56	[4]		3.4	[5]		2.1	[5]		1.37	[7]		–0.80	318 $\ell$	...
MRC B0625–536	06	26	22.14	–53	41	27.1	56	2		113	[2]		26	[5]		11.60	[4]		6.7	[5]		3.70	[32]		2.1	[7]		–1.03	118 $\ell$	1
MRC B0625–354	06	27	06.83	–35	29	14.0	18	2		33	[13]		9.2	[31]		5.86	[4]		4.88	[14]		2.90	[9]		2.27 <sup>i</sup>	[14]		–0.61	118 $\ell$	...
MRC B0625–545	06	26	47.21	–54	32	38.9	12.1:	2		...	...		7.9	[31]		5.00	[4]		3.2	[34]		1.73	[32]		0.93	[7]		–0.80	330 $\ell$	–4
MRC B0637–752	06	35	45.73	–75	16	15.8	12.5	2		20	[2]		7.89	[3]		6.67 <sup>i</sup>	[4]		5.33	[14]		5.16	[14]		5.36	[14]		–0.22	13 m	90
MRC B0646–398	06	48	11.30	–39	57	07.3	13.9	2		26	[13]		7.0	[5]		3.85	[4]		2.63	[18]		1.53	[9]		1.03	[7]		–0.80	82 d	–5
MRC B0647–475	06	48	48.36	–47	34	28.0	5.8:	2		...	...		4.35	[3]		3.22	[4]		...	...		1.14	[32]		0.68	[7]		–0.71	≤10 m	...
MRC B0658–656	06	58	12.84	–65	44	53.3	11.0	2		17	[2]		6.14	[3]		3.20	[4]		2.2	[11]		1.10	[21]		0.59	[7]		–0.91	25 m	90
MRC B0700–473	07	02	09.13	–47	26	33.5	9.2	2		14	[13]		4.33	[3]		1.85	[4]		1.1	[5]		0.60	[32]		0.27	[7]		–1.05	40 m	–56

Table 5—Continued

(1)	(2)	(3)	(4)	(5)	(6)	(7)	(8)	(9)	(10)	(11)	(12)	(13)		
Source	RA (J2000)	Dec	Flux density (Jy)			Flux density (Jy)			Flux density (Jy)			$\alpha_{408}^{2700}$	LAS <sup>a</sup>	P.A.
name	h m s	° ' "	$S_{178}$	$S_{80}$	$S_{408}$	$S_{843}$	$S_{1400}$	$S_{2700}$	$S_{5000}$		"	°		
MRC B0704–427	07 05 54.19	−42 48 54.4	9.6 2	21 [13]	4.47 [3]	2.32 [4]	1.5 [5]	0.8 [5]	0.35 <sup>i</sup> [7]	−0.92	37 m	−72		
PKS B0707–35	07 09 22.3	−36 02 11	9.1 1	15 [8]	4.6 [23]	3.42 <sup>i</sup> [22]	2.01 [22]	0.8 [5]	0.486 [35]	−0.93	486 e	−57		
MRC B0715–362	07 17 05.8	−36 21 41	10.6 2	18 [8]	5.7 [23]	3.78 [10]	2.32 [14]	1.27 <sup>i</sup> [14]	0.73 <sup>i</sup> [14]	−0.80	450 $\ell$	74		
MRC B0719–553	07 20 14.63	−55 25 16.4	11.9 2	24 [2]	5.63 [3]	3.54 [4]	2.0 [5]	1.22 [32]	0.76 [7]	−0.81	52 m	−24		
MRC B0743–673	07 43 32.44	−67 26 28.7	13.0: 1	...	...	8.61 [3]	5.55 [4]	5.3 <sup>i</sup> [11]	2.74 [21]	−0.61	14 m	−89		
MRC B0842–754	08 41 26.52	−75 40 32.4	30 2	58 [2]	13.35 [3]	6.45 [4]	4.3 [11]	2.15 [12]	1.37 [7]	−0.97	12 m	...		
MRC B0842–835	08 37 15.12	−83 44 41.4	11.0: 1	...	...	4.78 [3]	2.52 [4]	1.0 [11]	0.64 [12]	−1.06	12 m	9		
MRC B0846–811	08 43 38.82	−81 18 27.9	10.3: 2	...	...	4.09 [3]	1.94 [4]	1.1 [11]	0.50 [12]	−1.11	26 m	−50		
MRC B0906–682	09 06 52.43	−68 29 40.0	12.9: 2	...	...	6.11 [3]	3.04 [1]	1.7 [11]	0.89 [21]	−1.02	≤10 m	...		
MRC B0910–636	09 12 01.60	−63 52 39.1	9.2: 1	...	...	4.01 [3]	1.94 [4]	1.1 [11]	...	−0.99 <sup>b</sup>	≤10 m	...		
MRC B0943–761	09 43 23.98	−76 20 10.4	9.6: 2	...	...	4.91 [3]	2.86 <sup>j</sup> [1]	2.1 [11]	1.10 [12]	−0.79	≤10 m	...		
MRC B1003–415	10 05 57.40	−41 48 51.1	6.2 2	9 [13]	4.07 [3]	2.47 [4]	...	...	1.01 [9]	−0.74	≤10 m	...		
MRC B1015–314	10 18 09.29	−31 44 13.4	15 2	18 [13]	9.67 [3]	5.49 [1]	3.83 [18]	2.22 [16]	1.40 <sup>i</sup> [19]	−0.78	≤10 m	...		
MRC B1017–421	10 19 44.90	−42 24 53.7	11.6 2	27 [13]	5.04 [3]	2.18 [4]	1.7 <sup>i</sup> [5]	0.77 [9]	0.39 [7]	−0.99	88 d	−61		
MRC B1017–325	10 20 11.62	−32 45 33.9	9.3 2	14 [13]	4.76 [3]	2.69 [4]	1.79 [15]	1.00 [16]	0.54 [16]	−0.83	≤10 m	...		
MRC B1017–426	10 20 03.77	−42 51 31.5	23 2	42 [13]	12.72 [3]	6.61 [4]	4.20 [18]	2.33 [9]	1.45 [7]	−0.90	≤10 m	...		
MRC B1030–340	10 33 13.02	−34 18 43.7	12.7 2	28 [13]	5.59 [3]	2.40 [4]	1.4 [5]	0.64 [16]	0.29 [16]	−1.15	≤10 m	...		
MRC B1036–697	10 38 28.97	−70 03 08.8	11.1: 2	...	...	6.92 [3]	4.18 [4]	2.4 [11]	1.40 [21]	−0.85	≤10 m	...		
MRC B1044–357	10 46 45.06	−36 01 28.1	9.2 1	19 [13]	4.15 [3]	2.13 [4]	1.32 [15]	0.66 [9]	0.38 [9]	−0.97	53 m	−22		
MRC B1046–409	10 48 38.19	−41 13 57.2	9.6 2	19 [13]	5.02 [3]	2.76 [4]	...	...	1.38 [9]	−0.68	≤10 m	...		
MRC B1056–360	10 58 51.6	−36 19 46	6.9 2	12 [8]	4.09 [33]	2.40 [10]	...	...	0.96 [9]	−0.77	480 $\ell$	−21		
MRC B1116–462	11 18 26.94	−46 34 15.1	8.2 2	14 [13]	4.68 [3]	3.61 [4]	2.53 [14]	1.62 [14]	1.31 [14]	−0.56	15 m	79		
MRC B1123–351	11 25 54.46	−35 23 19.7	11.3 2	20 [13]	6.61 [33]	3.59 [4]	2.53 [14]	1.56 [14]	0.95 [14]	−0.76	60 d	87		
MRC B1136–320	11 39 17.17	−32 22 33.2	14 2	31 [13]	6.78 [3]	3.41 [4]	2.30 <sup>i</sup> [18]	1.16 [16]	0.65 [19]	−0.93	62 m	−16		
MRC B1143–483	11 45 31.08	−48 36 10.1	13.5 1	16 [13]	7.47 [3]	4.14 [4]	2.69 [18]	1.82 [36]	1.32 [7]	−0.75	≤10 m	...		
MRC B1143–316	11 46 20.55	−31 57 14.5	12.7 3	19 [13]	5.77 [3]	2.47 [4]	1.42 [20]	0.73 [16]	0.33 [19]	−1.09	46 m	82		
MRC B1151–348	11 54 21.79	−35 05 28.9	11.6 3	7 [13]	10.90 [3]	7.66 <sup>j</sup> [1]	6.33 [14]	4.37 [14]	2.70 [14]	−0.49	≤10 m	...		

Table 5—Continued

(1)	(2)	(3)	(4)	(5)	(6)	(7)	(8)	(9)	(10)	(11)	(12)	(13)		
Source	RA (J2000)	Dec	Flux density (Jy)			Flux density (Jy)			Flux density (Jy)			$\alpha_{408}^{2700}$	LAS <sup>a</sup>	P.A.
name	h m s	° ' "	$S_{178}$	$S_{80}$	$S_{408}$	$S_{843}$	$S_{1400}$	$S_{2700}$	$S_{5000}$		"	°		
MRC B1206–337	12 08 39.70	–34 03 05.0	10.6 2	17 [13]	4.65 [3]	2.18 [4]	1.11 [15]	0.48 [16]	0.22 [16]	–1.20	≤10 m	...		
MRC B1215–457	12 18 06.23	–46 00 28.6	12.8 2	16 [13]	9.59 [3]	6.74 <sup>j</sup> [1]	4.62 [18]	3.2 [5]	2.4 [7]	–0.59	≤10 m	...		
MRC B1221–423	12 23 43.37	–42 35 31.8	7.2 3	8 [13]	5.08 [3]	3.30 [4]	2.47 [14]	1.70 [14]	1.00 [14]	–0.59	≤10 m	...		
MRC B1232–416	12 35 41.96	–41 53 17.0	10.1 3	16 [13]	5.33 [3]	3.00 [1]	1.87 [14]	0.91 [9]	0.49 [14]	–0.94	≤10 m	...		
MRC B1234–504	12 37 15.28	–50 46 23.6	8.9: 1	...	...	4.57 [3]	2.86 <sup>j</sup> [1]	...	...	0.63 [7]	–0.80 <sup>b</sup>	≤10 m	...	
MRC B1243–412	12 45 57.56	–41 28 44.9	9.2 2	19 [13]	4.40 [3]	2.38 [4]	1.48 [37]	0.89 [9]	0.72 <sup>i</sup> [7]	–0.85	≤10 m	...		
MRC B1246–410	12 48 49.23	–41 18 38.6	23 2	44 [13]	10.59 [3]	6.37 [4]	3.91 [14]	2.21 [9]	1.29 [14]	–0.83	23 m	–88		
MRC B1247–401	12 50 05.92	–40 26 25.8	12.6 3	18 [13]	6.03 [3]	2.56 [4]	1.5 [5]	0.61 [9]	0.32 [7]	–1.21	≤10 m	...		
MRC B1259–769	13 03 12.38	–77 11 58.7	9.5: 1	...	...	4.15 [3]	1.89 [4]	1.2 <sup>i</sup> [11]	0.56 [12]	0.37 [7]	–1.06	≤10 m	...	
MRC B1259–445	13 02 30.7	–44 46 49	8.8: 1	...	...	4.2 [5]	2.19 [10]	1.7 <sup>i</sup> [5]	0.9 [5]	0.47 [7]	–0.82	132 d	37	
PKS B1302–325	13 04 56.1	–32 50 12	10.7: 2	18 <sup>i</sup> [13]	5.3 [31]	2.42 [10]	...	...	0.70 [16]	0.34 [16]	–1.07	342 e	32	
MRC B1302–491	13 05 27.8	–49 28 06	17 2	20 [8]	12.6 [27]	8.30 [10]	7.57 [14]	5.46 [14]	3.95 [14]	–0.45	510 $\ell$	40		
MRC B1303–827	13 08 39.45	–82 59 35.5	12.3: 1	...	...	4.84 [3]	2.11 [4]	1.3 [11]	0.58 [12]	0.55 <sup>i</sup> [7]	–1.12	15 m	–26	
MRC B1315–460	13 18 30.04	–46 20 34.9	9.3: 2	...	...	6.24 [3]	3.59 [1]	2.65 <sup>i</sup> [38]	1.32 [38]	0.63 [7]	–0.83	≤10 m	...	
PKS B1318–434	13 21 10.3	–43 42 40	12.3: 2	...	...	10.0 [23]	7.16 [10]	5.8 <sup>i</sup> [38]	3.09 [9]	1.71 [9]	–0.62	1020 $\ell$	37	
MRC B1320–446	13 23 04.14	–44 52 32.6	9.6: 2	...	...	6.91 [3]	4.61 [4]	...	...	1.79 [9]	0.99 [7]	–0.71	≤10 m	...
MRC B1322–427 <sup>d</sup>	13 25 31.8	–43 00 05	5553 1	8700 [8]	2740 [38]	2107 <sup>h</sup> ...	1330 [38]	912 [39]	579 [40]	–0.59	... e	...		
MRC B1330–328	13 33 35.89	–33 05 18.8	7.7 2	14 [13]	4.27 [3]	2.53 [4]	1.74 [15]	1.09 [16]	0.65 [16]	–0.72	23 m	1		
PKS B1333–33	13 36 38.8	–33 59 02	53 2	70 [8]	30.8 [23]	14.9 [10]	7.0 [5]	3.11 [14]	1.95 <sup>i</sup> [14]	–1.23	1920 $\ell$	–47		
MRC B1346–391	13 49 51.22	–39 22 48.5	13.8 2	32 [13]	5.84 [3]	2.97 [4]	1.85 [15]	0.98 [9]	0.56 [7]	–0.94	19 m	28		
MRC B1355–416	13 59 00.16	–41 52 51.3	24 2	37 [13]	12.9 [41]	7.33 [4]	4.6 [20]	2.49 [9]	1.54 [7]	–0.87	53 d	–59		
MRC B1358–493	14 01 31.59	–49 32 35.1	13.0: 1	...	...	6.46 [3]	3.74 [4]	...	...	0.85 [7]	–0.82 <sup>b</sup>	51 d	–48	
MRC B1359–358	14 02 40.13	–36 03 49.8	8.8 3	15 [13]	4.47 [3]	2.56 [1]	1.5 [5]	0.79 [9]	0.42 [17]	–0.92	≤10 m	...		
PKS B1400–33 <sup>e</sup>	14 04 05.8	–34 04 55	22: 2	52 [42]	5.8 [23]	1.3 [43]	0.46 [43]	...	...	...	...	960 $\ell$	35	
MRC B1407–425	14 10 29.09	–42 46 55.9	10.8 2	23 [13]	4.67 [3]	2.10 [4]	...	...	0.57 [9]	0.28 [7]	–1.11	23 m	...	
MRC B1413–364	14 16 33.67	–36 40 54.1	11.3 2	23 [13]	5.71 [33]	3.27 [4]	2.32 [14]	1.38 [9]	0.93 <sup>i</sup> [14]	–0.75	174 d	40		
MRC B1416–493	14 20 03.42	–49 35 45.0	11.1 2	12 [13]	7.34 [3]	3.84 [4]	2.42 [14]	1.3 [5]	0.95 <sup>i</sup> [14]	–0.93	40 m	54		
MRC B1421–382	14 24 16.53	–38 26 49.9	15 1	35 [13]	6.92 [3]	3.60 [4]	2.30 [20]	1.20 [9]	0.76 [7]	–0.93	61 d	–37		

Table 5—Continued

(1)	(2)	(3)	(4)		(5)		(6)		(7)		(8)		(9)		(10)	(11)	(12)	(13)	
Source	RA (J2000)	Dec					Flux density (Jy)									$\alpha_{408}^{2700}$	LAS <sup>a</sup>	P.A.	
name	h m s	° ' "	$S_{178}$		$S_{80}$		$S_{408}$		$S_{843}$		$S_{1400}$		$S_{2700}$		$S_{5000}$		"	°	
MRC B1421–490	14 24 32.20	−49 13 50.5	16:	1	...	...	13.10	[3]	9.92	[1]	8.81	[14]	7.08	[14]	5.41	[14]	−0.33	≤10 m	...
MRC B1424–418	14 27 56.29	−42 06 21.2	9.9	2	17	[13]	6.39	[3]	4.25 <sup>j</sup>	[1]	3.20	[18]	2.63	[9]	2.8 <sup>i</sup>	[7]	−0.47	≤10 m	...
MRC B1425–479	14 28 57.2	−48 12 02	13.0	2	29	[8]	4.5	[31]	1.46	[10]	...	...	...	...	0.061	[7]	−1.73 <sup>b</sup>	270 ℓ	52
MRC B1445–468	14 48 28.87	−47 01 41.5	16	3	14	[44]	6.97	[3]	3.06	[4]	1.79	[20]	1.1	[5]	0.59	[7]	−0.99	30 m	43
MRC B1451–364	14 54 28.50	−36 40 01.3	20	2	41	[8]	9.0	[31]	4.34	[4]	2.3	[20]	1.27	[9]	0.65	[19]	−1.04	123 d	−24
MRC B1458–391	15 01 34.79	−39 18 40.0	10.3:	1	...	...	6.07	[3]	3.88 <sup>j</sup>	[1]	2.9	[15]	...	...	1.27	[7]	−0.63 <sup>b</sup>	≤10 m	...
MRC B1526–423	15 30 14.30	−42 31 53.2	44	2	84	[13]	17.86	[3]	8.67	[4]	5.08	[18]	2.6	[34]	1.18	[7]	−1.02	50 m	−72
MRC B1540–730	15 46 07.51	−73 10 50.0	9.9:	2	...	...	5.33	[3]	2.88	[4]	1.8	[11]	0.92	[21]	0.49	[7]	−0.93	42 m	86
MRC B1540–337	15 44 02.91	−33 52 29.3	8.5	2	17	[13]	4.33	[3]	2.56	[4]	1.72	[15]	0.97	[16]	0.63	[16]	−0.79	42 m	48
MRC B1545–321	15 48 59.0	−32 17 01	32:	1	...	...	9.0 <sup>h</sup>	...	3.58	[22]	1.64	[22]	0.81	[16]	0.29	[16]	−1.41 <sup>c</sup>	420 e	−36
MRC B1547–795	15 55 22.30	−79 40 37.5	21:	2	...	...	10.45	[3]	6.13	[4]	4.0	[11]	2.28	[12]	1.48	[7]	−0.81	38 m	17
MRC B1549–790	15 56 58.91	−79 14 03.8	7.5:	2	...	...	7.95	[3]	6.62 <sup>j</sup>	[1]	...	...	4.65	[14]	3.20	[14]	−0.29	≤10 m	...
MRC B1607–841	16 19 34.05	−84 18 18.9	11.2:	2	...	...	4.91	[3]	2.53	[1]	1.7	[11]	0.69	[12]	0.43	[7]	−1.04	≤10 m	...
MRC B1610–771	16 17 49.50	−77 17 18.1	5.4:	2	...	...	5.35	[3]	4.80 <sup>j</sup>	[1]	5.0	[11]	4.16	[14]	3.47	[14]	−0.13	≤10 m	...
MRC B1622–310	16 25 55.41	−31 08 07.9	10.0	2	17	[13]	5.20	[3]	2.95 <sup>i</sup>	[4]	1.71	[15]	1.06	[16]	0.65	[19]	−0.84	≤10 m	...
MRC B1633–681	16 38 10.46	−68 14 08.6	16:	1	...	...	6.66	[3]	3.11	[4]	1.3 <sup>i</sup>	[11]	0.91	[21]	0.47	[7]	−1.05	60 d	−24
MRC B1637–771	16 44 18.5	−77 15 40	24:	1	...	...	13.5	[11]	8.18	[10]	6.5	[11]	4.37	[14]	3.02	[14]	−0.60	330 ℓ	−10
MRC B1655–776	17 02 41.51	−77 41 57.1	9.6:	2	...	...	5.04	[3]	3.09	[4]	2.5	[11]	1.43	[12]	1.05	[14]	−0.67	21 m	−88
MRC B1706–606	17 10 29.73	−60 41 17.5	12.9:	1	...	...	5.54	[3]	2.87	[4]	...	...	...	...	0.46	[7]	−1.01 <sup>b</sup>	11 m	78
MRC B1716–800	17 25 25.68	−80 04 45.4	12.7:	2	...	...	5.91	[3]	3.50	[4]	2.5	[11]	1.11	[12]	0.76	[7]	−0.88	43 d	−54
MRC B1721–836	17 33 55.37	−83 42 53.3	13.0:	1	...	...	4.63	[3]	1.62	[4]	1.0	[11]	0.22 <sup>i</sup>	[12]	0.19	[7]	−1.61	≤10 m	...
PKS B1733–56 <sup>f</sup>	17 37 35.76	−56 34 14.9	41:	1	...	...	20.3	[23]	12.56	[4]	8.17	[14]	4.63	[14]	3.37	[14]	−0.79	269 d	38
MRC B1737–575	17 41 30.81	−57 37 15.3	10.8:	1	...	...	5.12	[3]	2.89	[4]	...	...	1.17	[32]	0.65	[7]	−0.78	15 m	−69
MRC B1737–609	17 42 01.6	−60 55 21	16:	1	...	...	8.32	[3]	3.91	[10]	3.3	[11]	2.0	[34]	1.09	[7]	−0.75	78 d	−33
MRC B1740–517	17 44 25.42	−51 44 43.9	3.7:	2	...	...	5.38	[3]	6.55 <sup>j</sup>	[1]	...	...	4.60	[32]	3.6	[7]	−0.08	≤10 m	...
MRC B1754–597	17 59 06.31	−59 46 59.6	20	2	25	[2]	12.58	[3]	5.88	[4]	3.9	[5]	1.5	[5]	0.73	[7]	−1.14	21 m	39
MRC B1756–663	18 01 17.96	−66 23 02.9	11.6:	1	...	...	5.46	[3]	3.02	[4]	...	...	1.05	[21]	0.60	[7]	−0.87	≤10 m	...

Table 5—Continued

(1)	(2)	(3)	(4)		(5)		(6)		(7)		(8)		(9)		(10)		(11)	(12)	(13)
Source	RA (J2000)	Dec							Flux density (Jy)								$\alpha_{408}^{2700}$	LAS <sup>a</sup>	P.A.
name	h m s	° ' "	$S_{178}$	$S_{80}$	$S_{408}$	$S_{843}$	$S_{1400}$	$S_{2700}$	$S_{5000}$										
MRC B1814–519	18 18 06.96	–51 58 09.6	24 3	27 [2]	14.26 [3]	6.51 [1]	3.54 [14]	1.6 [5]	0.63 [14]	–1.17	≤10 m	...							
MRC B1814–637	18 19 35.01	–63 45 48.1	71: 2	...	37.00 [3]	20.22 [1]	13.16 [14]	7.5 [5]	4.34 [14]	–0.85	≤10 m	...							
MRC B1817–391	18 20 35.31	–39 09 28.4	19 1	32 [13]	9.74 [3]	4.80 [4]	2.40 [15]	... ..	0.70 <sup>i</sup> [7]	–1.06 <sup>b</sup>	16 m	–41							
MRC B1817–640	18 22 16.10	–63 59 19.3	28: 1	...	11.50 [3]	4.70 [4]	2.6 [34]	1.43 [32]	0.82 [7]	–1.10	31 m	65							
MRC B1818–557	18 22 21.00	–55 41 52.6	9.5 1	23 [2]	4.14 [3]	2.17 [4]	... ..	0.71 [32]	0.45 [7]	–0.93	94 $\ell$	–44							
MRC B1819–673	18 24 34.91	–67 17 29.7	10.4: 1	...	6.06 [3]	3.74 [4]	2.1 [11]	1.65 [21]	1.14 [7]	–0.69	45 d	–28							
MRC B1827–360	18 30 58.90	–36 02 30.3	33 3	15 [13]	25.83 [3]	13.86 <sup>j</sup> [1]	7.2 [15]	3.2 [5]	1.28 [14]	–1.12	≤10 m	...							
MRC B1829–344	18 32 32.41	–34 22 38.8	9.6 1	23 [13]	4.19 [3]	2.55 [4]	1.61 [15]	0.88 [16]	0.45 [16]	–0.83	25 m	...							
MRC B1831–668	18 36 59.32	–66 49 08.7	5.3: 2	...	4.28 [3]	3.41 [4]	... ..	1.24 [21]	0.74 [7]	–0.66	11 m	...							
MRC B1839–487	18 43 15.47	–48 36 37.8	18 1	28 [13]	9.08 [3]	5.88 [4]	3.13 [18]	2.0 [5]	1.35 [7]	–0.81	62 $\ell$	...							
MRC B1840–404	18 44 28.35	–40 21 55.8	16 2	30 [13]	8.44 [3]	4.78 [4]	2.50 [20]	1.6 [5]	0.95 [7]	–0.89	46 d	–61							
MRC B1853–303	18 57 10.56	–30 19 41.1	10.9 1	22 [13]	5.09 [3]	2.74 [4]	1.66 [15]	0.93 [16]	0.49 [16]	–0.90	19 m	30							
MRC B1854–663	18 59 58.02	–66 15 02.2	8.0: 2	...	4.41 [3]	2.53 <sup>j</sup> [1]	1.2 [11]	0.87 [21]	0.44 [7]	–0.86	≤10 m	...							
MRC B1917–546	19 21 52.87	–54 31 55.0	13.0 2	27 [2]	4.59 [3]	1.37 [4]	0.9 <sup>i</sup> [5]	0.18 [36]	0.050 [7]	–1.71	36 m	–33							
MRC B1922–627	19 27 27.28	–62 39 34.4	8.0 2	12 [2]	4.88 [3]	3.04 [4]	2.31 [14]	1.22 [14]	0.70 [14]	–0.74	66 d	57							
MRC B1923–328	19 26 28.28	–32 42 42.9	10.2: 2	...	4.25 [3]	2.18 [4]	1.23 [15]	0.60 [16]	0.34 [16]	–1.04	34 m	78							
MRC B1929–397	19 33 23.83	–39 40 23.7	11.2 2	17 [13]	6.41 [33]	4.18 [4]	2.69 [29]	1.54 [9]	0.98 [7]	–0.75	105 d	–56							
MRC B1932–464	19 35 57.10	–46 20 41.7	80 2	154 [13]	39.61 [3]	21.20 [4]	12.85 [14]	6.72 [14]	3.43 [14]	–0.94	19 m	–74							
MRC B1933–587	19 37 32.37	–58 38 27.8	14 2	17 [2]	9.13 [3]	4.56 [1]	3.5 [5]	1.55 [36]	0.95 [7]	–0.94	≤10 m	...							
MRC B1934–638	19 39 25.08	–63 42 45.5	0.63:3	...	6.24 [3]	13.65 [1]	16.12 <sup>i</sup> [14]	11.37 <sup>i</sup> [14]	6.26 <sup>i</sup> [14]	0.32	≤10 m	...							
MRC B1940–406	19 43 51.87	–40 30 10.2	14 1	27 [13]	5.7 [23]	2.61 [4]	1.6 [5]	0.49 <sup>i</sup> [9]	0.14 <sup>i</sup> [7]	–1.30	126 d	–11							
MRC B1953–425	19 57 15.22	–42 22 20.1	18 2	29 [13]	10.13 [3]	5.53 [4]	3.22 [18]	1.60 [9]	0.93 [7]	–0.98	≤10 m	...							
MRC B1954–552	19 58 16.64	–55 09 39.7	31 2	54 [2]	14.8 [5]	9.70 [4]	6.29 [14]	3.91 [14]	2.37 [14]	–0.71	360 $\ell$	35							
MRC B1955–357	19 59 03.75	–35 34 31.9	8.9 2	15 [13]	4.86 [3]	2.80 [1]	1.71 [18]	1.10 [9]	0.67 [19]	–0.79	≤10 m	...							
MRC B2006–566	20 10 19.1	–56 27 03	35 2	81 [2]	12.2 [5]	5.5 [45]	2.38 [14]	... ..	0.40 <sup>i</sup> [14]	–1.36 <sup>b</sup>	1680 $\ell$	–30							
MRC B2009–524	20 13 21.12	–52 18 09.5	8.3 2	14 [2]	4.52 [3]	2.44 [4]	1.8 [5]	1.1 [5]	0.66 [7]	–0.76	18 m	–71							
MRC B2013–557	20 18 01.0	–55 39 30	10.3 2	19 [2]	4.8 [23]	2.43 [10]	1.82 <sup>i</sup> [29]	0.7 [5]	0.53 <sup>i</sup> [24]	–1.03	1200 $\ell$	–23							
MRC B2020–575	20 24 20.70	–57 23 39.2	20 2	36 [2]	9.89 [3]	5.16 [4]	3.7 [5]	1.9 [5]	1.18 [7]	–0.88	66 d	24							

Table 5—Continued

(1)	(2)			(3)	(4)		(5)		(6)		(7)		(8)		(9)		(10)	(11)	(12)	(13)			
Source	RA (J2000)			Dec							Flux density (Jy)							$\alpha_{408}^{2700}$	LAS <sup>a</sup>	P.A.			
name	h	m	s	°	'	''	$S_{178}$	$S_{80}$	$S_{408}$		$S_{843}$	$S_{1400}$	$S_{2700}$	$S_{5000}$				"	°				
MRC B2028–732	20	33	50.62	−73	04	07.7	9.5	2	18	[2]	4.57	[3]	2.47	[4]	1.6	[11]	0.74	[21]	0.42	[7]	−0.96	78 d	56
MRC B2031–359	20	34	44.55	−35	48	50.8	9.0	2	18	[13]	4.40	[3]	2.55	[4]	1.72	[15]	0.93	[9]	0.67	[9]	−0.82	22 m	0
MRC B2032–350	20	35	47.66	−34	54	02.5	27	2	44	[13]	17.60	[3]	9.06	[4]	5.40	[18]	3.40	[9]	1.88	[19]	−0.87	26 m	−3
MRC B2041–604	20	45	20.72	−60	19	01.3	27	2	55	[2]	11.16	[3]	4.87	[4]	2.8	[11]	0.9	[5]	0.41	[7]	−1.35	32 d	47
MRC B2049–368	20	52	17.50	−36	40	29.8	11.4	2	19	[8]	5.75	[3]	2.66	[1]	1.4	[5]	0.65	[9]	0.316 <sup>i</sup>	[35]	−1.15	≤10 m	...
MRC B2052–474	20	56	16.31	−47	14	47.1	7.1	2	14	[13]	4.15	[3]	2.30 <sup>ij</sup>	[1]	2.37	[18]	2.2	[5]	2.0	[7]	−0.34	≤10 m	...
MRC B2059–641	21	03	26.35	−63	56	51.2	9.3	2	17	[2]	4.24	[3]	1.87	[4]	0.9	[11]	0.51	[32]	0.24	[7]	−1.12	19 m	−64
MRC B2115–305	21	18	10.68	−30	19	14.7	11.4	2	18	[13]	6.89	[3]	3.89	[4]	2.54	[15]	1.50	[14]	0.87	[14]	−0.81	12 m	−39
MRC B2122–555	21	26	15.08	−55	21	14.2	8.7	2	17	[2]	4.05	[3]	2.74	[4]	...	...	0.89	[32]	0.63	[7]	−0.80	18 m	...
MRC B2128–315	21	31	23.24	−31	21	12.1	8.1	3	12	[13]	4.18	[3]	2.25	[4]	1.18	[46]	0.80	[16]	0.48	[16]	−0.87	≤10 m	...
MRC B2140–434	21	43	33.46	−43	12	48.5	19	2	32	[13]	9.18	[3]	5.17	[4]	2.72	[18]	1.66	[9]	0.98	[7]	−0.90	56 d	−5
MRC B2140–817	21	47	23.96	−81	32	11.7	26:	2	...	...	8.72	[3]	5.02	[4]	3.1	[11]	1.57	[12]	1.07	[7]	−0.91	44 m	−20
PKS B2148–555	21	51	27.2	−55	20	32	11.6:	1	...	...	5.8	[31]	2.45	[10]	...	...	0.87	[32]	0.48	[7]	−1.00	780 $\ell$	26
MRC B2150–520	21	54	07.47	−51	50	15.0	18	2	28	[2]	10.08	[3]	5.43	[4]	4.2 <sup>i</sup>	[5]	2.1	[5]	1.19	[7]	−0.84	15 m	−34
MRC B2152–699	21	57	06.91	−69	41	24.3	93:	1	...	...	61.6	[23]	37.30	[4]	26.6	[47]	18.29	[14]	13.40	[21]	−0.65	70 d	18
MRC B2153–699 <sup>g</sup>	21	57	47.95	−69	41	53.4	29:	1	...	...	11.9 <sup>h</sup>	...	5.26	[4]	3.4	[47]	...	...	...	...	...	27 d	24
MRC B2158–380	22	01	15.13	−37	46	39.8	8.3	2	21	[13]	4.12	[3]	2.41	[4]	...	...	1.01	[9]	0.64	[7]	−0.74	97 d	51
MRC B2201–555	22	05	04.89	−55	17	43.3	13.1:	1	...	...	5.56	[3]	3.06	[1]	2.1 <sup>i</sup>	[5]	0.90	[6]	0.50	[7]	−0.96	≤10 m	...
MRC B2213–456	22	16	55.46	−45	21	43.7	6.2	2	8	[13]	4.33	[3]	2.79	[4]	1.82	[18]	1.08	[6]	0.65	[7]	−0.73	≤10 m	...
MRC B2223–528	22	27	02.69	−52	33	25.4	17	2	30	[2]	8.83	[3]	4.17	[4]	3.0 <sup>i</sup>	[5]	1.35	[6]	0.74	[7]	−0.99	11 m	−72
MRC B2226–411	22	29	18.47	−40	51	31.7	11.3	2	19	[13]	6.83	[3]	4.43	[4]	2.72	[18]	1.85	[9]	1.05	[7]	−0.69	≤15 m	...
MRC B2226–386	22	29	46.90	−38	23	59.2	14	3	13	[13]	8.21	[3]	3.81	[1]	2.07	[15]	0.88	[9]	0.40	[7]	−1.18	≤10 m	...
MRC B2250–412	22	53	03.41	−40	57	46.4	26	2	47	[13]	13.93	[3]	6.93	[4]	4.46	[18]	2.34	[9]	1.43	[7]	−0.94	20 m	80
MRC B2252–530	22	55	50.13	−52	45	42.4	12.1	2	22	[2]	6.37	[3]	3.85	[4]	3.2 <sup>i</sup>	[34]	1.66	[6]	1.00	[7]	−0.71	≤10 m	...
MRC B2253–522	22	56	47.53	−51	58	41.5	15:	1	...	...	7.20	[3]	3.75	[4]	3.1 <sup>i</sup>	[5]	1.30	[6]	0.78	[7]	−0.91	11 m	...
MRC B2259–375	23	02	23.86	−37	18	05.8	13.0	3	15	[13]	7.47	[3]	4.30	[1]	2.69	[18]	1.53	[9]	0.99	[7]	−0.84	≤10 m	...
MRC B2305–418	23	07	52.74	−41	32	45.1	7.5	3	11	[13]	4.02	[3]	2.15	[4]	1.46	[18]	0.83	[9]	0.50	[7]	−0.83	≤10 m	...



Table 5—Continued

(1)	(2)	(3)	(4)	(5)	(6)	(7)	(8)	(9)	(10)	(11)	(12)	(13)
Source	RA (J2000)	Dec	Flux density (Jy)							$\alpha_{408}^{2700}$	LAS <sup>a</sup>	P.A.
name	h m s	° ' "	$S_{178}$	$S_{80}$	$S_{408}$	$S_{843}$	$S_{1400}$	$S_{2700}$	$S_{5000}$		"	°
MRC B2319–550	23 22 06.84	−54 45 29.8	13.2: 1	⋯ ⋯	5.73 [3]	2.90 [1]	2.2 <sup>i</sup> [5]	0.89 [6]	0.50 [7]	−0.99	≤10 m	⋯
MRC B2323–407	23 26 34.12	−40 27 17.8	15 2	26 [13]	9.28 [3]	5.21 [1]	3.33 [18]	1.78 [36]	1.19 [7]	−0.87	≤10 m	⋯
MRC B2331–416	23 34 26.13	−41 25 25.1	30 2	51 [13]	15.92 [3]	8.26 [4]	5.26 [14]	2.66 [9]	1.66 [14]	−0.95	19 m	53
MRC B2332–668	23 35 11.29	−66 37 04.6	12.7 2	26 [2]	5.93 [3]	3.27 [4]	2.5 <sup>i</sup> [11]	1.27 [21]	0.81 [7]	−0.82	28 m	−43
MRC B2338–585	23 41 18.36	−58 16 10.3	15 2	25 [2]	8.17 [3]	4.13 [4]	3.3 <sup>i</sup> [5]	1.38 [36]	0.98 <sup>i</sup> [7]	−0.94	≤10 m	⋯
MRC B2339–353	23 41 45.87	−35 06 22.4	10.3 2	15 [13]	5.67 [3]	3.19 [1]	1.82 [15]	0.91 [9]	0.46 [9]	−0.97	≤10 m	⋯
MRC B2354–350	23 57 00.91	−34 45 34.7	23 3	52 [13]	8.70 [3]	3.00 [4]	1.30 [18]	0.35 [9]	0.117 <sup>i</sup> [35]	−1.70	68 m	−39
PKS B2356–61	23 59 00.46	−60 54 44.4	148 2	296 [2]	61.2 [23]	38.90 [4]	25.80 [14]	16.00 [14]	9.71 [14]	−0.72	378 e	−45

<sup>a</sup>Size flags: (d) separation of peaks of a double source; (e) largest separation of peaks of a complex source; ( $\ell$ ) largest size of low-surface-brightness emission in a complex source: the position angle given is that of the central axis; (m) deconvolved extent along the axis of a source, as in JM92.

<sup>b</sup>Spectral index defined between 408 and 5000 MHz.

<sup>c</sup>Spectral index defined between 843 and 5000 MHz.

<sup>d</sup>The total angular extent is almost 10° (e.g. Cooper et al. 1965), whereas that of the inner lobes is 6'.8 (JM92). The position angle of the structure varies at different angular scales: for the inner lobes it is 49° (JM92).

<sup>e</sup>The position, largest angular extent and position angle are the 408 MHz values from McAdam & Schilizzi (1977).

<sup>f</sup>The position is that of the core in the MOST image.

<sup>g</sup>Angular size and position angle were measured from an ATCA contour map (Norris et al. 1990), as the MOST CUTS were affected by MRC B2152–699.

<sup>h</sup>Flux density estimated from the radio spectrum.

<sup>i</sup>Flux density not used in estimating  $S_{178\text{MHz}}$ .

<sup>j</sup>Variable at 843 MHz (Gaensler & Hunstead 2000).

References. — (1) Campbell-Wilson & Hunstead (1994); (2) Mills et al. (1961); (3) Large et al. (1981); (4) this paper; (5) Bolton et al. (1964); (6) Wright et al. (1977); (7) Gregory et al. (1994); (8) Mills et al. (1960); (9) Bolton & Shimmins (1973); (10) JM92; (11) Price & Milne (1965); (12) Shimmins & Bolton (1972b); (13) Slee (1995); (14) Wills (1975); (15) Condon et al. (1998); (16) Shimmins & Bolton (1974); (17) Shimmins & Bolton (1972a); (18) Fomalont & Moffet (1971); (19) Shimmins et al. (1969); (20) Fomalont (1968); (21) Bolton & Butler (1975); (22) Subrahmanyam et al. (1996); (23) SM75; (24) Wall & Schilizzi (1979); (25) Quiniento et al. (1988); (26) Saripalli et al. (1994); (27) Cameron (1971); (28) Goldstein (1962); (29) Smith (1983); (30) Clarke et al.

(1976); (31) Molonglo Transit Catalogue; (32) Wall et al. (1975); (33) Ekers et al. (1989); (34) Gardner et al. (1969); (35) Wright et al. (1996); (36) Shimmins (1971); (37) Quiniento & Echave (1990); (38) Cooper et al. (1965); (39) Rogstad & Ekers (1969); (40) Junkes et al. (1993a), reduced by 15% (Alvarez et al. 2000); (41) Wyllie (1969b); (42) McAdam & Schilizzi (1977); (43) Subrahmanyam et al. (2003); (44) Slee & Higgins (1973); (45) Röttgering et al. (1997); (46) Quiniento & Cersosimo (1993); (47) Christiansen et al. (1977).

Table 6. Sample size, source density, and median values of various quantities for sources in the MS4, SMS4, and 3CRR samples.

(1) Sample	(2) N	(3) Source density (sr <sup>-1</sup> )	(4) Median values	
			$S_{178}$ (Jy)	$\alpha$
MS4	228	$94.0 \pm 6.2$	$12.1^{+0.6}_{-0.7}$	$-0.86^{+0.03}_{-0.02}$
SMS4	137	$56.5 \pm 4.8$	$15.7^{+0.5}_{-0.7}$	$-0.91^{+0.04}_{-0.02}$
3CRR	172	$40.6 \pm 3.1$	$15.6^{+0.8}_{-0.8}$	$-0.81^{+0.03}_{-0.01}$